Spectrochimica Acta Part B 101 (2014) 269–287

Contents lists available at ScienceDirect

Spectrochimica Acta Part B

journal homepage: www.elsevier.com/locate/sab

Review

A review of the development of portable laser induced breakdown spectroscopy and its applications

J. Rakovský [a,*], P. Čermák [b], O. Musset [c], P. Veis [b]

[a] J. Heyrovský Institute of Physical Chemistry, Academy of Sciences of the Czech Republic, Dolejškova 3, 18223 Prague 8, Czech Republic
[b] Department of Experimental Physics, Faculty of Mathematics, Physics and Informatics, Comenius University, Mlynská dolina F2, 842 48 Bratislava, Slovakia
[c] Laboratoire interdisciplinaire Carnot de Bourgogne, UMR CNRS 6303, Université de Bourgogne, BP 47 870, F-21078 Dijon Cedex, France

ARTICLE INFO

Article history:
Received 12 May 2014
Accepted 13 September 2014
Available online 23 September 2014

Keywords:
Laser-induced breakdown spectroscopy
Portable LIBS
Fieldable LIBS
Fiber laser
Microchip laser

ABSTRACT

In this review, we present person-transportable laser induced breakdown spectroscopy (LIBS) devices that have previously been developed and reported in the literature as well as their applications. They are compared with X-ray fluorescent (XRF) devices, which represent their strongest competition. Although LIBS devices have advantages over XRF devices, such as sensitivity to the light elements, high spatial resolution and the possibility to distinguish between different layers of the sample, there are also disadvantages and both are discussed here. Furthermore, the essential portable LIBS instrumentation (laser, spectrograph and detector) is presented, and published results related to new laser sources (diode-pumped solid-state, microchip and fiber lasers) used in LIBS are overviewed. Compared to conventional compact flashlamp pumped solid-state lasers, the new laser sources provide higher repetition rates, higher efficiency (less power consumption) and higher beam quality, resulting in higher fluences, even for lower energies, and could potentially increase the figure of merit of portable LIBS instruments. Compact spectrometers used in portable LIBS devices and their parts (spectrograph, detector) are also discussed.

Contents

1. Introduction

When an intensive laser pulse that is focused onto a sample surface is absorbed by the surface, a small amount of the material can be removed (ablated), vaporized and ionized to finally form a plasma

* Corresponding author.
E-mail address: jozef.rakovsky@jh-inst.cas.cz (J. Rakovský).

http://dx.doi.org/10.1016/j.sab.2014.09.015
0584-8547/

plume that emits light. The light has a characteristic spectral structure relating to the plasma and the sample composition. The ablation abilities and plasma formation after the interaction of the intensive laser pulse with a material surface have been observed very soon after the invention of the laser. This knowledge, combined with optical emission spectroscopy methods, later resulted in a new analytical technique: laser induced breakdown spectroscopy (LIBS) [1]. Over the past 50 years, thousands of articles, a handful of books [2–8] and a number of reviews [9–29] have been published dealing with LIBS fundamental [9,10,15,16,30], archeological [14], biomedical [26] and geological applications [18], instrumentation and methodology [17,27], fieldable LIBS [11], remote LIBS [25], single pulse LIBS [21] and the LIBS of light elements in steel [19] or in non-conducting materials [20]. Special attention should be paid to Hahn's and Omenetto's extensive two-part review [16,17] which contains close to one thousand references.

The usefulness of LIBS under laboratory conditions has been proven and presented many times since the first application. However, there has always been a demand for sample analysis in the field from where the samples originate. This could increase the speed of the analyses which could be crucial, for example, when analyzing dangerous chemical agents or explosives. Sometimes the nature of the sample does not allow it to be transported to the laboratory. In any case, the elimination of the process of both transporting and storing the sample, and therefore speeding up the analysis, is itself a highly motivating factor in the effort to increase the portability of these analytical devices. Of course, a certain degree of miniaturization of the device depends on the analysis type, relating to some technical implementation, and this is not always possible with the current level of technologies. In 1996, Yamamoto et al. [31] presented design possibilities for a portable LIBS instrument and commenced the development of portable LIBS devices.

As it turns out, recently, the possibilities of miniaturizing LIBS into really lightweight and portable instruments, operated by persons with a minimal training, are in progress. For example, this is seen in the effort to introduce a real handheld LIBS device onto the market by private companies that weighs a couple of kilograms, is easily portable and provides analytical results within a few seconds. Progress is possible due to the miniaturization of the lasers, spectrometers, and computers accompanied by the miniaturization of the electronics and the increase in the storage capacities of the batteries powering the devices.

In 2010, Laserna and Fortes [11] published a review on fieldable LIBS devices, covering most of the fieldable devices developed until the year the review was published. The devices were separated into three groups, whereby for this review the portable LIBS group is the most important one. The goal of this review is to help orientate the reader in the area of portable LIBS instruments and relating publications to those instruments that push the borders toward a higher level of portability. With respect to the interest in a higher level of portability for LIBS devices, the instruments that meet certain additional criteria are described. These criteria naturally appear when someone has to carry the instrument in the field, particularly areas that cannot be reached by a car or with a trolley. With higher portability in mind, the LIBS devices presented here meet the criteria for maximum weight and how they are powered. In this review, we focus on the instruments that weigh up to a maximum of 15 kg, can be carried by one person over a short distance, and with an ability to overcome certain barriers: e.g. stairs. Moreover, the instrument should be powered by batteries; however, there are two exceptions to this: the first portable LIBS instrument [31] and the device developed by Laserna et al. [32–36]. Although there are other possibilities for powering the devices in the field, such as portable generators or solar cells, the use of batteries offers high portability, something that the aforementioned power sources cannot offer.

Dimensions, weight and power consumption are key features for portable instruments. These parameters depend on the most important parts of the device: the laser and spectrometer. Up until now, flashlamp pumped solid state lasers (FLPSS) were commonly used in the devices. However these days, new laser sources represented by small diode-pumped solid-state (DPSS), microchip and fiber lasers are available for use in LIBS devices. The lasers rapidly improve their performance and although they have been already used in LIBS studies, suggesting their usefulness in portable LIBS devices, they are not widely used. The authors of this work hypothesize that implementation of the new laser sources in the devices could help to further progress in the portable LIBS area. Therefore, the present article provides a review of published results relating to LIBS studies dealing with the new laser sources, followed by a discussion that addresses their usefulness. The spectrometer is another important part of the instrument, the parameters of which strongly influence the figure of merit of the overall instrument. Although there have not been as many technological improvements compared to the laser sources, we discuss the spectrographs and detectors that can help in the design of the portable LIBS instrument.

2. Notes on the portable LIBS instrumentation

Portable LIBS devices are commonly composed of a probe and a control unit (see Fig. 1). The sample is examined by the probe part which is held in the hand. In order to make the probe part lightweight, with acceptable dimensions, the probe part and control part are separated and placed in two different boxes. The probe part contains a laser and collecting optics. The other part, such as a spectrometer, computer, electronics, batteries, pump or gas purge, and which do not need to be placed close to the laser, are placed in the control unit box. Thus for spectral analyses of laser induced plasma (LIP), the light is collected in the probe and delivered to the spectrometer in the control unit via an optical fiber. The obtained spectra are further treated by the computer, which is also located in the control unit.

For the devices reviewed in Table 2, there are two versions of the probe and two versions of the control unit. Fig. 1 shows the possible configurations of the probes, called type 1 and type 2. Type 1 is destined for general use whereas type 2 is more suitable for the analysis of samples located on a floor or high on a wall. It can have a longer reach due to the longer laser light path to the focusing lens (type 2a) or by placing the laser with a focusing lens on a long handle (type 2b).

Fig. 1 also presents four common configurations of the collecting optics, labeled A–D. In A–C, the collected light is focused onto the fiber and therefore the light only contains spatially limited spectral information about a portion of the volume of the LIP plume. Conversely, in the case of D, the light is spatially integrated from the LIP volume given that the light entering the fiber is only limited by an angle described by the numerical aperture of the fiber. The spatial integration of the light also means that there is a spatial integration of parameters such as the temperature and density of the different LIP species, which may make it difficult to interpret these parameters. They are more meaningful for the spectra originating from a small LIP volume and are important, for example, in calibration free analyses. Although the interpretation of these parameters is not important for most of the portable LIBS devices, a collecting optics is used as it can result in a higher signal due to more light being collected. This can be important, especially for weak emission lines.

The two versions of the control units used are shown in Fig. 2. The backpack version can be considered as being more portable than the suitcase version. An interesting design of the portable LIBS instrument was presented in [37], where the instrument parts are integrated within a multi-pocketed flak vest.

The laser and spectrometer are two key parts of the LIBS system and their performance influences the capabilities of the overall instrument. Unlike laboratory systems and bigger portable or transportable LIBS systems, in this review, the laser's and spectrometer's performance is limited due to the weight and dimension restrictions. Therefore, the question regarding a compromise in the laser's and spectrometer's parameters is more essential.

The laser's function is to initiate the breakdown, ablate sample material, heat it and form the plasma plume. These processes are induced by the intensive laser pulse, focused onto the sample surface and of course,

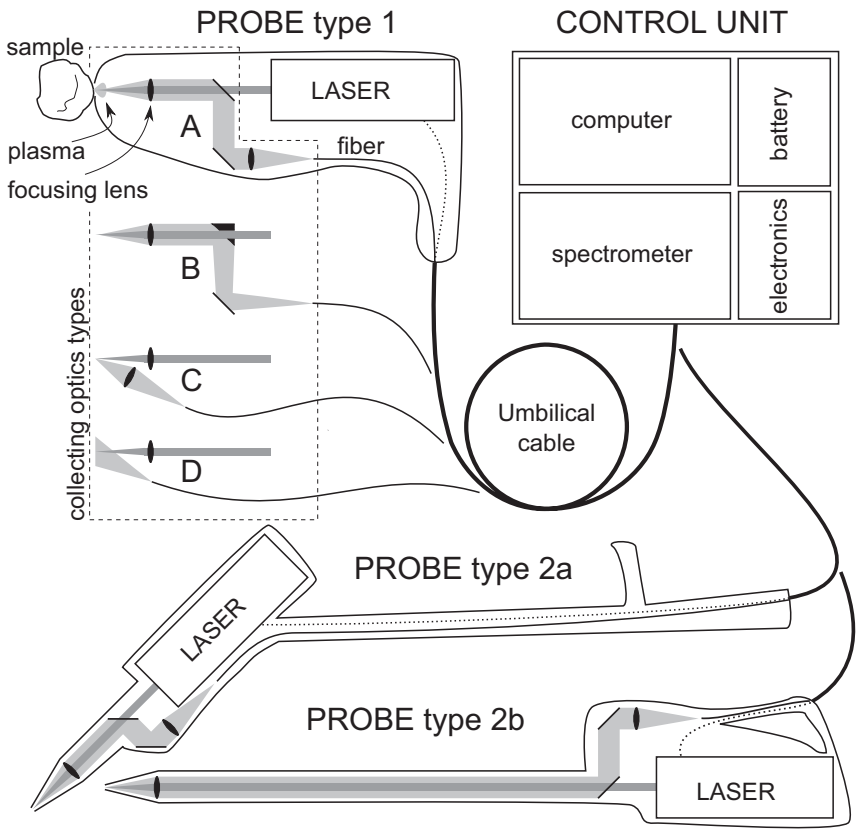

Fig. 1. Two main parts of the portable LIBS instrument: PROBE and CONTROL UNIT with their parts. Two versions of the probes are shown: PROBE type 1, with a more general concept, and PROBE type 2, used more specifically for samples located on a floor or on a wall, which are easier and more comfortable to reach. There are different collecting optic configurations used for plasma light collection to the optical fiber: A — the first mirror is transparent for laser wavelengths but reflects collecting plasma light, B — focusing mirror with a hole in the center for laser light, C — the plasma light is simply focused by the collecting lens and D — no collecting lens is used and plasma light is immediately collected by the fiber.

the efficiency of these processes is dependent on the parameters of the laser. For LIBS applications, the energy per pulse is an important parameter; however, the energy of the laser pulse per area (cm^2) or of the laser pulse per time (second) per area (cm^2) is more meaningful and produces quantities called fluence (J/cm^2) and power density (W/cm^2), respectively. These quantities are dependent on the laser's focus spot size and are higher for a smaller spot. This means that even small low energy lasers can produce high fluence pulses if they have good focusing ability. The laser's focusing ability is dependent on the laser beam quality, which is usually expressed by a beam quality factor M^2. M^2 equal to one means a perfect Gaussian beam, for which the focusing ability is limited only by the diffraction. A two-fold larger M^2 results in a two-fold larger attained spot size diameter and four-time lower fluence or power density. Another important parameter is the repetition rate of the laser. It describes the number of pulses generated by the laser per second (Hz). With higher repetition rates, the number of detected spectra increases and the measurement time decreases.

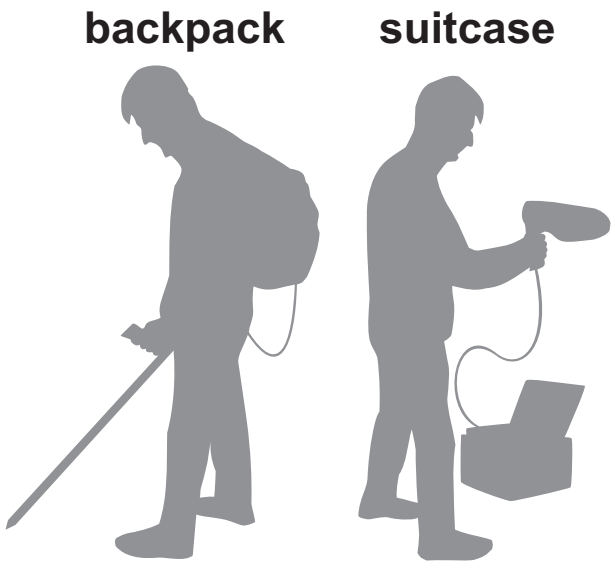

Fig. 2. Illustration of two of the most widely used implementations of the control unit for portable LIBS devices: backpack and suitcase.

In LIBS, the interaction of the laser pulse with the sample material is usually described by the breakdown threshold and the ablation efficiency. The breakdown threshold depends on the sample material, with typical values on the order of several Joules per square centimeter for the nanosecond laser pulses [28,38]. The ablation efficiency is usually expressed by a volume or mass of the ablated material per pulse energy. Typical values for some metals for a nanosecond laser source are 0.03–0.2 $\mu m^3/J$ [39]. It is worth mentioning that both the breakdown threshold and the ablation efficiency depend on the laser's parameters, for instance, pulse duration, wavelength and beam quality. For a more detailed description of the laser's interaction with the sample surface, the reader is asked to consult Ref. [40].

After plasma induction is achieved, the role of the spectrometer is to record the intensity of the emitted light as a function of its frequency. This emission spectrum contains information about the sample/gas composition (presence of atomic lines) as well as information describing the parameters of the induced plasma (e.g. electron density or temperature). There are three main parameters describing the performance of the spectrometer: (i) spectral range, (ii) resolution, and (iii) acquisition timing.

When dealing with the spectral range of the spectrometer, ideally we would like to have a system capable of covering the emission of all possible elements present in the generated plasma with sufficient resolution to unambiguously distinguish between the different transitions. Fig. 3 was created in order to gain an idea of what these requirements mean. Here, an overview of the emission line intensities was plotted as a function of their wavelength. The selection of the elements for Fig. 3 was based on the elements targeted by the portable devices described in this review and represents an overview of the elements commonly targeted by LIBS devices. For each element, both emission lines from the neutral and firstly ionized states are represented in the lower and upper part of the corresponding row, respectively. The transition data were collected from the NIST [41] and Kurucz's [42] atomic spectra database. A simulation was performed for an arbitrary temperature value — 1 eV. Finally, the spectra were synthesized by representing each transition by the Gauss peak function with the full width of 0.2 nm. It is worth emphasizing that the spectra are theoretical, assuming a Local Thermal Equilibrium (LTE) and optically thin plasma, and can differ from real LIBS spectra. The difference may be most significant for the intensive lines due to self-absorption. In order to help the reader, the most intensive transitions with a final state energy below 0.1 eV are indicated with a dark triangle, representing potentially self-absorbed transitions.

A second aspect of the spectroscopic performance is the resolution, described by the resolving power R equal to the ratio $\lambda/\Delta\lambda$, where $\Delta\lambda$ is the line width at the wavelength λ. In LIBS, this parameter is driven by two aspects most of the time: (i) the capability to resolve two close transitions and (ii) the ability to retrieve additional plasma parameters such as the electron concentration from the line shape of the transitions. The former aspect is nicely demonstrated in the study carried out by Cremers et al. [76]. Their goal was to measure atomic transitions from two isotopes of the same atom. They took measurements on two Argon lines at 419.1 nm separated by 0.032 nm and on two Uranium lines at 424.4 nm separated by 0.025 nm. In order to discriminate between these two transitions, they compared two spectrometers providing an R of 44,000 and 75,000, respectively. Most of the time, there is no need for such high resolution and values that are up to ten times lower are sufficient for most of the LIBS measurements.

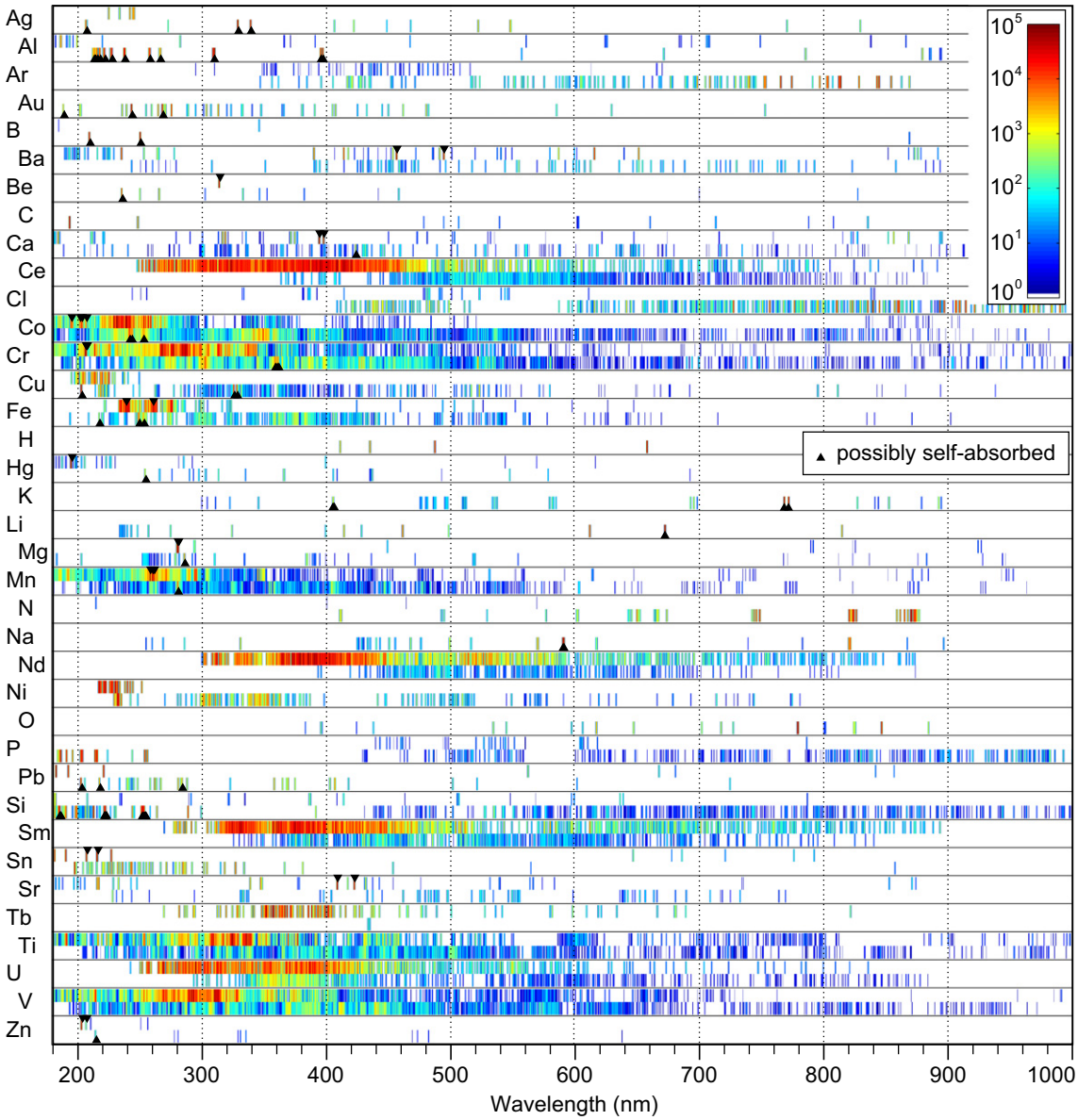

Fig. 3. LIBS spectra of the elements studied in the reviewed publications relating to portable LIBS devices. The spectra are theoretical, modeled for optically thin plasma in local thermodynamic equilibrium with temperature of 1 eV. For each element, the neutral (bottom) and single ionized atom (top) transition lines are shown separated. The overall element spectra are normalized (to the value 10^5) and plotted in logarithmic scale. The triangles mark most intensive lines which could be self-absorbed and thus their real intensity could be much lower.

Regarding the specificity of LIBS applications, the most critical parameters are the acquisition timing and the synchronization of the detector(s). This comes from the very fast evolution of the LIP parameters as well as from their dynamical range. To gain a quantitative perspective, we review two recent works [43,44] dealing with this problem. In both works, the authors used gated detectors to precisely determine the time evolution of the plasma temperature and electron density and their implications for the LTE in the LIP. Aguilera and Aragón [44] studied LIP in pure nitrogen and over a glass substrate during the first 10 μs after the laser pulse, focusing on the atomic and ionic emissions. They used a 60 mJ energy pulse with a duration of 4.5 ns at 1064 nm at atmospheric pressure. In both cases, the evolution of the studied parameters was similar and followed the plasma expansion theory with the temporal decrease as $t^{-6/5}$ in the first 0.5 μs after the laser pulse. In this one half of a microsecond, the plasma temperature, as measured from the Boltzmann distribution of the atomic ad ionic lines, dropped from 4.3 eV to about 1.3 eV. The electron density, following the same decrease rate, fell from about 7.0×10^{18} cm^{-3} to about 1.0×10^{18} cm^{-3}. In the following period of time, the cooling of the LIP was mainly radiative. After 1 μs, the parameters were decreasing almost linearly, the temperature fell from 1.2 to 0.86 eV (8 μs after the laser pulse) and the electron density dropped from about 2.0×10^{17} cm^{-3} to about 5.0×10^{16} cm^{-3} (at 4 μs after the laser pulse). Lam et al. [43] studied LIP with similar techniques but over a different sample — an Al_2O_3 target doped with titanium (Ti) and iron (Fe). In addition, their investigation covered much larger time scales — up to 100 μs after the laser pulse and the temperature was also determined from the shape of the AlO rotational-vibrational spectra. With regard to the first 10 μs of the LIP, they obtained very similar results to those previously described (both for electron density and the temperature retrieved from the atomic and ionic lines). Over a longer time scale, when the presence of AlO spectra allowed for the determination of the rotational temperature (starting from approximately 30 μs after the laser pulse), the authors found that the condition for LTE was not fulfilled, as the value of this temperature was close to 3000 K smaller than the excitation temperatures for the electronic states. Summarizing these results, we can conclude that in order to record the whole plasma emission, an integration time up to hundreds of microseconds may be needed. This case would be very similar to the spatial integration of the signal, where by summing the emissivity from whole space the signal-to-noise (S/N) ratio can be increased. On the other hand, if a detailed analysis of the plasma needs to be performed (e.g. in the calibration-free measurements), the window for the spectral observation is narrowed. Ideally our target is the time of LIP expansion where radiation cooling is dominant and the LTE condition is fulfilled. According to the two disused works, this corresponds to times from about 1 to 10 μs, with integration widths on the μs scale. A comparison between gated and non-gated detectors is discussed in more detail in Section 5.2.2.

3. LIBS vs. XRF portable devices

Most frequently, the LIBS technique, intended for field applications, is compared with the X-Ray Fluorescence (XRF) spectroscopy technique, which is strong competitor of LIBS. Although XRF is the method of choice for many field applications, the LIBS technique has some advantages over XRF and vice versa. However, combining XRF and LIBS instruments can be effective and was also presented in Ref. [45–47]. For a fast comparison of both techniques, some of their features are overviewed in Table 1.

In principle, XRF can detect elements with an atomic number as low as beryllium ($Z = 4$); however in practice, the detection of elements lighter than magnesium ($Z = 12$) is limited [26,48]. Primarily, this is due to a low fluorescence yield for the light elements and an attenuation by the air environment [19,49]. Unlike XRF, LIBS can basically detect all elements on the periodic table [50]. Generally, elements from laser induced plasma emit a lot of lines in the UV, VIS or NIR region and provide a possibility to avoid or minimize interference from different spectral lines. Conversely, the XRF spectrum only contains a couple of (at least one) lines per element so that the interference could cause a problem due to the lack of alternative lines, especially in complex matrices (e.g. As in the presence of Pb) [31].

Since in LIBS, a laser pulse is focused onto a small spot on the sample surface, an ablated material and induced plasma originate from this small area (~0.01 mm^2) and therefore the spatial resolution of LIBS is high. The focusing of X-rays is more difficult and the area irradiated by conventional XRF devices is usually much larger (~100 mm^2) [51] and the spatial resolution is smaller. The spatial resolution of LIBS devices is usually reported as an advantage over the spatial resolution of XRF devices. However, X-ray focusing is already possible using a polycapillary lens or doubly curved crystal optics. Nowadays, they are implemented in new generation devices termed μXRF or Micro X-ray with a spatial resolution higher than 100 μm [52]. They are even implemented in commercial transportable and handheld μXRF devices [53,54]. Actually, a high spatial resolution is not so critical for portable devices if the device needs to be held in the hand. Moreover, it can become a disadvantage in the case of inhomogeneous samples, where spatial integration over a larger area is required, and consequently can extend the time of measurement. To investigate a larger sample area in LIBS, the geometry of the focusing optics can be modified by using a cylindrical focusing lens, producing a line-shaped spark, instead of the common spherical lens [28,31,55,56]. Another possibility is to use a micro-lens array [57,58], characterized by a very good repeatability of the LIBS spectra.

The time consumption of both techniques is difficult to compare as there are many factors that need to be taken into consideration. However, a single LIBS spectrum can be obtained in a fraction of a second, whereas it takes at least a couple of seconds to get the XRF spectrum. From this point of view, the first pieces of information are obtained faster by LIBS than by XRF.

Table 1
Brief comparison of some features of the LIBS and XRF techniques. The "x" marks features that are better for LIBS.

		LIBS	XRF
Element detection range	x	All	From Na to heavier
Isotope detection	x	Partly	No
Line interference in spectra	x	Lower — lot of lines	Higher — few lines
Lateral spatial resolution	x	Higher — small focus	Lower — large focus
Depth spatial resolution	x	High	No
Sensitivity to surface contamination	x	Low — cleaning shots	High
Sensitivity to sample inhomogeneity		Higher	Lower
Sample destructivity		Partly destructive	Non-destructive
Analysis rapidity	x	Higher	Lower
Analysis precision		Lower	Higher
Analysis difficulty		Higher — complex spectra	Lower — simple spectra
Safety	x	Safety glasses	X-ray source — safety rules about manipulation and transportation

Table 2
Overview of portable LIBS devices and their parameters with related references.

Ref.	Weight, realization	Laser	Spectrometer	Samples, elements (LOD)
[31] I.	Suit case 46 × 33 × 24 cm 14.6 kg 115 V AC	Kigre MK-367 Laser Photonics MYLA Nd:YAG, 1064 nm Passive Q-switch 15–20 mJ/pulse 1 Hz (0.5 Hz) 50 mm focusing lens	Oriel MultiSpec f = 1/8 m; 25, 50, 100 μm slits; 2400 L/mm grating; 250 nm blaze CCD 256 × 1024 pixels Almost axial, no collection lens	Paint Pb (8000) Soil Ba(265), Be(9.3), Pb(298), Sr(42) Filters + Be particles size μm (LOD ng/cm^2) >6(63), 2.5–663(63), 0.9–1.7(31), <0.4(21) filters + Pb particles 0.5–5 μm (5.6 μg/cm^2)
[62] II.	Suit case 48.3 × 33 × 17.8 cm 13.8 kg Battery	Kigre MK-367 Nd:YAG, 1064 nm Passive Q-switch 21 mJ/pulse 1/3 Hz (0.25 Hz) 20 mm focusing lens	Ocean Optics S2000 2400 L/mm 339–462 nm 0.4 nm resolution linear CCD 2046 pixels Trigger, but not used Axial, collection lens	Paint Pb (1200 ppm) NIST steel Mn (160 ppm) NIST ores Mn NIST organics samples Ca(1300 ppm)
[63,64] III.	Aluminum case 23 × 51 × 38 cm Battery and 115 V DC	Kigre MK-367 Nd:YAG, 1064 nm Passive Q-switch 15 mJ/pulse 0.25 Hz 45 mm focusing lens	f = 1/6 m, 2400 L/mm 250 nm blaze 0.35 nm resolution Cooled CCD 250 × 12, 24 μm pixel 20 nm spectral range Not triggered Almost axial, no collection lens	Paint Pb, soil Pb (100 ppm) Ti, Fe, Sr, Zn, Al
[32–36] IV	Backpack 45 × 23 × 15 cm 5 kg +hand-held probe With PDA wireless control +laser power supply and water cooling unit	Ultra CFR, Big Sky Laser, Quantel Nd:YAG, 1064 nm Q-switch 50 mJ/pulse 10 Hz 75.6 mm focusing lens	Ocean Optics HR2000 2400 L/mm 240–340 nm 370–460 nm 0.05 nm resolution Linear CCD 2048 pixels Directly into fiber (d = 500 μm, NA = 0.22)	[35] Malaga cathedral: Al, C, Ca, Cu, Fe, Mg, Si, Ti [32] speleothems.: Al, C, Ca, Fe, Mg, Mn, Si, Ti [33] lead in road sediments: Al, Ca, Fe, Pb (190 μg/g), Si, Sr, Ti [34] oil spill residues: Al, C, Ca, H, N, O, Mg, Na, Fe, Si, V [36] stalagmite slabs: Al, C, Ca, Mg, Si, Sr
[68–70] V	Backpack 40 cm long hand-held probe, heads-up display Battery	ALST, Inc. Nd:YAG, 1064 nm Active Q-switch 50 mJ/pulse 0.5 Hz	Ocean Optics LIBS3000 7 channels 200–980 nm 0.1 nm resolution CCD Axial, collection lens	[68] *Bacillus globigii* [70] landmines detections [69] soil, quartz
[80,81,83,84] VI.a VI.b	Porta-LIBS-2000 Suit case 18 × 33 × 46 cm 14.5 kg Battery	Kirge MK-367 Nd:YAG, 1064 nm Passive Q-switch 25 mJ/pulse 1 Hz	Up to 6 channels 200–1000 nm 0.1, 0.2 nm resolution Used in configuration: Two StellarNet EPP2000 LSR 14 μm slits 200–600 nm 0.2 nm resolution Linear CCD 2048 10 delay possibilities	[83] C in soil [84] Cu in soil LOD 2.3 mg/dm^3, precision 0.5 (mg/dm^3)^2 Artificial Neural Network
[37] VII.	Integrated in a multi-pocketed flak vest Battery	Modified Kigre MK-830 DPSS Er: glass 1535 nm Active Q-switch 10 mJ/pulse 10 Hz 6 mm focusing lens	Three Stellarnet EPP2000 (200–800 nm) Avantes AvaSpec-2048- USB2 193–465 nm Ocean Optics S2000 Testing 2pc Stellarnet EPP2000 200–600 nm With/without collecting lens	Steel standard, aluminum standard, pyrophyllite mineral standard, terbium glass standard, barium phosphate glass standard, europium phosphate glass standard, lithium silicate glass standard, uranium silicate glass standard and four rocks with unknown composition, Al, B, Ba, Ca, Ce, Co, Cr, Fe, Mg, Mn, N, Na, Nd, O, P, Si, Sm, Tb, Ti, U
[50,85,86] VIII.	LIBSCAN 25, 25+ Hand-held probe 34 × 21.5 × 10 cm, 2 kg Instrument console 41 × 28 × 16 cm, 12–15 kg Battery	Nd:YAG, 1064 nm Passive Q-switch 50 mJ/pulse 1 Hz 3 lens adjustable beam expender	Up to 6 channels: 185–256 nm, 0.05 nm res. 255–315 nm, 0.05 nm res. 314–416 nm, 0.05 nm res. 414–498 nm, 0.03 nm res. 496–718 nm, 0.15 nm res. 716–904 nm, 0.15 nm res.	[86] gunshot residue, Au, Ba, Ca, K, Mg, Sn, Sr, Ti [50] home-made explosives, Ammonium nitrate, Sodium chlorate, Ar, Cl, N, O [85] ancient greave, Ag, Al, Au, Cu, Fe, Mn
[60,78] IX.	Two parts: an optical gun (30 × 23 × 12 cm) and a compact analyzing box +26 × 19 × 9 cm <5 kg battery or 230 V AC	Lab-made Nd:YAG 1064 nm Active Q-switch Up to 45 mJ/pulse 1 Hz 50 mm focusing lens after telescope ×2	Ocean Optics HR2000+ 200–650 nm 0.4 nm resolution min. integration time 1 ms Delay −10 to +10 μs step 0.5 ns aspheric collecting lens	[78] brass, red pigment, Cu, Zn, Hg, Ca [60] geological samples, Al, Ba, Ca, Fe, Na, Ti

Table 2 *(continued)*

Ref.	Weight, realization	Laser	Spectrometer	Samples, elements (LOD)
[73,74] X.	Backpack 8.2 kg Battery	Kigre Mk-367 Nd:YAG, 1064 nm Passive Q-switch <25 mJ 0.3 Hz	3× Ocean Optics HR2000+ Approx. resolution 2000–3000	Magnets, steels, aluminum alloys, carbon fiber or graphite, Aramid rubber, uranium ore [73]
[79] XI.	Laser: 20 × 24 × 10 cm 3 kg Spect. 26 × 21 × 11 cm 2 kg Whole 7 kg Battery	Lab-made Nd:YAG 1064 nm Passive Q-switch Up to 45 mJ/pulse <5 ns	Lab-made 0.3 nm resolution 480–560 nm range CCD	Coin, Cu
[75,76] XII.	Backpack 10.4 kg Handheld probe 5 kg Battery	Kigre MK-367 JP Innovations DP5120 Nd:YAG, 1064 nm Active EO Q-switch 14 mJ/pulse <10 ns 10 Hz	EMU-65 (Catalina Scientific Instruments) Resolving power 44,000 200–1000 nm UV Luca R EMCCD 7.7 kg	U_3O_8 ($U^{238/235}$) UO_3, UO_2 and UF_4 U_3O_8 with Al, Ca, Cr, Cu, Mg, Na, V D, H Li

XRF is a completely non-destructive method, whereas LIBS is partly destructive. Every laser shot removes a fraction of a microgram of material from the sample surface and creates a small crater. This can be a problem in the case of valuable samples where any marks caused by the analysis are unacceptable, or if a sample is too small or too thin to obtain an appropriate spectra quality before completely destroying the sample.

On the contrary, the removal of material shot by shot can reveal information about the composition as a function of depth. In the case of XRF, the penetration length is not so clear. This LIBS feature was presented in [31,59] on paint samples where layers with different Pb content were well resolved. In [60], the possibility to determine the fossilization depth on ammonite shells was shown and in [32], the depth profile of the Sr/Ca intensity for a speleothem was determined.

As XRF contains a radioactive source, special handling precautions are needed. However, this can limit the ability to transport this device or possibly make it more complicated. For LIBS, there are no special operation restrictions, except for the wearing of protective eye glasses because of the laser. However, even this can be avoided by the use of an eye-safe Er:glass laser [37], which has already recently been implemented in a commercial portable LIBS device (Z 500 in Table 4).

A very recent comparison of the XRF and LIBS techniques can be found in Ref. [61], in which both systems were evaluated for the identification of various metallic alloy samples. The XRF system without a gas purge equipped with a polycapillary focusing lens was compared to the LIBS system with a fiber laser source and a small compact spectrometer. The results strongly suggest that the LIBS technique is more suitable, mainly due to the ability to identify the light elements and the ability to perform faster analyses.

4. Overview of the portable LIBS systems

An overview of the developed portable LIBS devices and their applications is presented in this section. Two types of publications are reviewed: publications relating either to non-commercial devices developed in research laboratories or to commercial devices developed by private companies and used by research laboratories for studies in the LIBS domain. A list of both device types with the related publications is shown in Table 2. This table contains twenty six publications relating to twelve devices that meet the restrictions of portable devices defined in the introduction (Section 1), except for devices I. and IV. Each row contains one portable LIBS instrument with a description of the main parameters and the related references. The devices are numbered from I. to XII. These numbers can also be found in Fig. 4 where the spectral ranges and resolution of the devices are presented graphically. A more detailed description of the devices is found below.

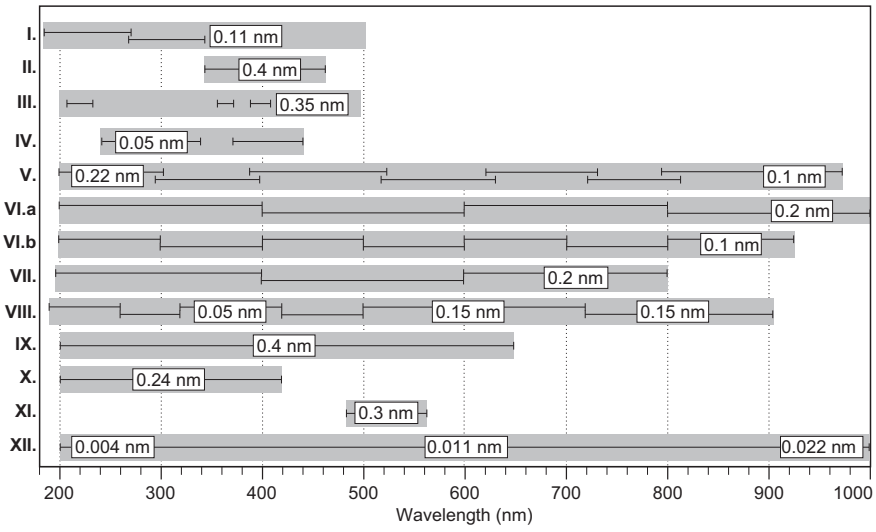

Fig. 4. Overview of spectrographs with their spectral range and the resolution used in different portable LIBS devices.

4.1. Laboratory prototypes

The first portable LIBS instrument was developed at the Los Alamos National Laboratory by Cremers et al. [31]. The instrument weighed 14.6 kg and was packed in a suitcase measuring 46 × 33 × 24 cm powered by 115 V AC. It was evaluated for measurements of Pb in paint, metals in soils and particles collected on filters. The authors pointed out the relationship between the energy of the laser and the limit of detection (LOD). When the energy of the laboratory laser system was six times higher, except for Sr, the LOD obtained with the portable instrument was higher by roughly the same factor. The advantages of LIBS compared to XRF were presented in the conclusion. The XRF device is an alternate choice to LIBS and for many applications, XRF is the device of choice. However as Cremers pointed out, there are also advantages and these are discussed in further detail in Section 3.

The first portable LIBS device proved that LIBS analyses could be performed in the field and was the prototype for the construction of the next portable LIBS instrument [62]. However, this instrument was already powered by a battery and therefore completely autonomic. The distance of the laser's focusing lens from the sample surface was optimized with respect to the signal-to-background (S/B) ratio via plasma imaging with an ICCD camera. The optimal distance for a 20 mm focal length lens was estimated to be 18.5 mm. An additional S/B ratio extension and more than one order increase in a S/N ratio were achieved through spatial filtering by an off-axis configuration for the collecting optics. The configuration enabled the collection of light from the plasma edge instead of its core. This effect was also previously described by Multari et al. [56] and it relates to the strong continuum fluctuation when the spectrum are detected non-triggered during the whole evolution of the plasma (see Section 5.2.2).

The problem with a strong continuum in non-triggered detection was also noticed in the LIBS spectra obtained by the second instrument [63,64], also based on Cremers et al.'s prototype [31]. As presented, detection with a 100 ns delay to the laser onset can improve the S/B ratio from 0.5 to 1.6. Surprisingly, the authors showed that the sensitivity of the two different systems, with lower and higher resolution, can be almost equal if the background can be estimated. However, it was difficult to estimate the background level with the low resolution system due to the emission of neighboring Ti lines. The portable system was applied to real field measurements of Pb in soil and Pb in paint on wood. Different temperatures for the exited electronic states of Pb and different LIBS signal variations were presented for metallic Pb, Pb in dry soil and Pb in moistened soil samples [64], suggesting that the nature of the sample has a strong influence on the parameters of the plasma. Moistened samples can cause serious problems in LIBS analyses, especially for low energy lasers, and was also mentioned in other works [65–67].

A different design from Cremers' prototype was used in Ref. [68]. The suitcase was replaced by a backpack, providing higher portability, and the probe was prolonged to reach samples located on the floor from a standing position. This design allowed a comfortable analysis on the ground, e.g. detection of *Bacillus globigii* from the floor. The system was also tested on a Quartz sample and a soil sample to compare its performance with the "sister" bench-top instrument [69]. The authors pointed out that in the case of poorly coherent materials containing aggregates of different particles (like soil or minerals), it is not possible to use simple spectra accumulation (averaging) in order to increase the S/N ratio. A single-shot spectra needs to be used for the identification instead. The capability of land mine identification by the portable LIBS system was evaluated in Ref. [70].

Next, two portable LIBS devices were developed by Laserna's group [32–36,71,72]. It should be mentioned that the devices are equipped with a 10 Hz FLPSS water cooled laser (Quantel Ultra CFR Big Sky laser operating at 1064 nm with 50 mJ/pulse energy), weighing about 15 kg with high power consumption, powered by 230 AC. One of the devices was designed as a backpack (45 × 23 × 15 cm, 5 kg in weight) containing all of the needed instruments except the laser. The other one was designed as a suitcase with wheels. If the devices used a smaller and lower power-consuming laser, they would meet the criteria for a portable instrument as defined in Section 1. As the backpack version is more portable, its application will be quickly discussed; however, it is suggested that the reader also reads the references relating to the suitcase version [71,72].

The backpack version was used to map the chemical composition of the facade of the Malaga cathedral [35], to study speleothem alteration layers inside the Nerja cave (a large karstic formation in southern Spain) [32], to determine lead in road sediments [33], to detect oil spill residues [34] and to study the spatial distribution of paleoclimatic proxies in stalagmite slabs [36]. In the initial study, the system was used for a real-time evaluation of the Si/Ca, Si/Mg and Ca/Mg ratios. This process allowed the identification of four different materials (sandstone, limestone, marble and cement mortar) used in the construction of the Malaga cathedral. In the next study, the aim was to perform an identification analysis of the speleothems' alteration layers as well as to evaluate the functionality of the instrument in harsh environments (low temperatures and high humidity). The instrument was able to measure the Sr/Ca depth profile up to 1250 μm in 90 s and can be considered as a worthwhile tool for studies on speleothem genesis. The system was also used for the quantitative analysis [33]. This was done inside the Cerrado de Calderon tunnel (in Malaga, Spain). The goal was to evaluate the Pb that was released from the traffic and deposited on the walls of the tunnel. Pb concentrations were calculated using the calibration curve obtained by laboratory measurements with the same LIBS system. A LOD of 190 μg/g was reached with an accuracy of 14%. In a recent application [36] of the device, a high correlation between LIBS and the ICP-AES lateral profile obtained from a speleothem was presented. The results suggest that the device can be a useful analytical tool, providing fast results.

To reach ground samples and samples located on walls, Barefield et al. [73,74] used a similar design for the LIBS instrument used in Ref. [68]. However, instead of using a prolonged laser path, they placed the laser closer to the sample using a longer handle. The backpack mounted portable system was essentially developed to detect actinides in safeguard applications. The system used the same laser source as the first three abovementioned systems. It was a very popular compact passively Q-switched Nd:YAG laser from KIGRE that produced approximately 25 mJ of energy per pulse with an operating repetition rate of 0.3 Hz. The laser source was used with a single HR2000 + spectrometer from Ocean Optics with a wavelength range and optical resolution of 200–420 nm and 2000–3000, respectively. The focusing and collecting parts were not precisely described but they were included, along with the laser, in a head at the end of a probe. The spectra were analyzed with a compact pocket computer. The whole system, which weighed approximately 8.2 kg, was battery powered with an operating time of 1.5 h. This system was used to analyze a lot of samples such as magnets, steel, aluminum alloys, carbon compounds and natural abundances of uranium in standard reference material. A multivariate analysis was used to identify or classify samples of similar types, however there is no detailed description about the results of the analysis.

The design with the prolonged laser path similar to the instrument described in Ref. [68] was also used by Cremers et al. [75] (see Fig. 5). The instrument was also composed of two parts: a backpack part weighing 10.4 kg and a handheld probe part weighing 5 kg. It is important to mention that the device has been recently upgraded by replacing the FLPSS by a DPSS laser with a repetition rate of 10 Hz [76]. Just by replacing the laser, the device provides over 30 times more LIBS spectra in a same time, even if the energy of the new laser is at least 50% lower than the energy of the old laser. Cremers' instrument was evaluated for isotopic measurements of U^{238} and U^{235} mixtures, the first time a portable LIBS instrument was used for such a difficult task. To distinguish two different isotopes, one has to resolve very close emission lines relating to the different isotopes with a different isotopic shift. In the previously reported laboratory LIBS measurements of uranium isotopic shifts, a reduced atmospheric pressure was used to narrow emission lines broadened by Stark's

Fig. 5. Picture of the portable LIBS instrument developed by Cremers et al. [76]. The device houses a DPSS laser with a repetition rate of 10 Hz.
Published with the permission of the Society for Applied Spectroscopy.

effect. However, Cremers et al. [76] pointed out that this is not the limiting factor for resolving uranium isotopes lines by LIBS and the limitation factor was attributed to the resolving power of the spectrometer used. The isotopic shift of uranium 238 and 235 for the UII 424.437 nm line is approximately 0.025 nm. To resolve the isotopic shift, two high resolution echelle type spectrometers were used. In order to circumvent the line broadening, a delay of 4 μs was used after the laser pulse before the spectra were detected. The first spectrometer, with higher resolution (6.8 pm), exhibited a clear possibility to completely resolve the two different isotope lines, with a high correlation between the nominal and measured uranium isotope ratios. However, the spectrometer was too bulky to consider it as portable. The second spectrometer was much smaller and more lightweight (~7 kg) and was therefore suitable for the portable instrument; however, the resolution was lower (10 pm). Using the second spectrometer, it was possible to distinguish the difference between 0.7% (natural), 50% and 93% enriched uranium. The instrument housing the lighter spectrometer can be considered as portable and is useful for uranium isotope ratio determination under ambient pressure in air. Cremers' instrument suggests that the implementation of a new kind of laser source and more powerful spectrometers can further push the use of portable LIBS systems toward more challenging applications.

In [77], Myers et al. presented a small compact eye-safe erbium glass DPSS laser for LIBS application with an output energy of 5 mJ per pulse and a repetition rate of 10 Hz. It was shown that the laser could possibly discriminate healthy and unhealthy human skin tissue. A similar DPSS laser (Kigre MK-830) and detecting system were used in a portable LIBS device developed by the same group [37]. The instrument was mainly assembled from commercially available parts placed in a multi-pocket flack vest and together with the abovementioned portable LIBS instrument used by Cremers, they were the only two portable LIBS instruments using a DPSS laser. However, the laser used by Myers was additionally lasing on 1.54 μm, which is what makes the laser eye-safe, and eye-protection glasses were not needed to operate the instrument. Interesting parts such as a hands-free near-eye display or a hand-held finger track mouse were used to control the device. The handheld laser was gun shaped and together with the other parts, this made the instrument highly portable. During the testing process, the authors presented the spectra recorded for different samples with peaks assigned to the different elements; however, a detailed analysis of the results is missing.

Although the DPSS laser seems to be better for portable LIBS applications, the work of Musset's group [60,78] indicates that even by using a flashlamp pumped laser, a portable LIBS device can be very compact with a full weight under 5 kg and an operation time up to 6.5 h. The laser presented by Goujon et al. in [78] was developed in the same laboratory and therefore was easier to adapt to the portable LIBS system [60]. The system comprised two main parts (see Fig. 6): a gun-shaped box, designed for comfortable handling, and a second box containing the spectrometer, the batteries and a computer. A small pump with a filter case was added to remove the dust produced during the laser ablation process. The connection between the two parts was made with an umbilical cable containing a fiber transmitting light to the spectrometer. The main part of the laser gun is an Nd:YAG actively Q-switched laser capable of producing up to 45 mJ of energy at a wavelength of 1064 nm with a repetition rate of 1 Hz. The laser gun contains all of the optical devices such as the focusing system (×2 telescope with a 50 mm converging lens) and the collection lens. There are two user screens, one for the video signal coming from the analyzing surface and a second showing the laser configuration. The spectrometer included in the second box is a commercial LIBS product Ocean Optics HR2000+ with spectral range of 200–650 nm. A small laptop with touch screen capability, connected to the spectrometer and to the laser by USB, is included in the second compact box. Two lab-made software were used to control the operating parameters of both the laser and spectrometer and to treat the acquired spectra in situ. Performances of the single broadband spectrometer with low resolution were analyzed and compared with a standard high resolution gate spectrometer to evaluate the limitations of the portable device. The system was tested on geological samples in the field to find volcanic ash layers (called tephra) in sediments or to sort fossils by identifying the fossilization processes [60]. The results were also compared to those obtained with a commercial mobile XRF.

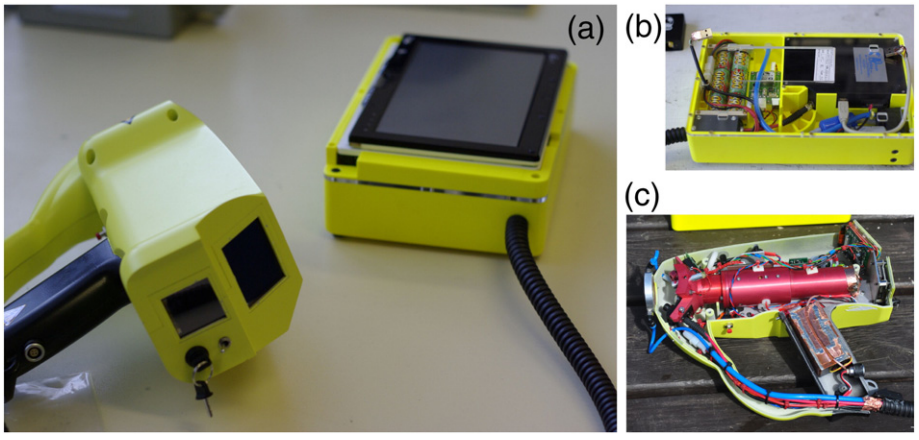

Fig. 6. (a) Picture of the portable LIBS instrument developed by Musset et al. [60,78], composed of two parts. (b) The control unit part contains the spectrometer, batteries, pump, filter and a small computer on top of the box (this can be seen in figure (a)). (c) The laser probe part contains a small FLPSS laser, focusing and collecting optics, a camera and two displays.

Studies on geological materials have shown the interest of punctual measurements and the very good ability to measure the presence of elements such as Barium, which are difficult to detect by XRF.

Another LIBS instrument for application in the Bolivian mining industry, equipped with a homemade laser, was developed by Ormachea et al. [79]. Again, the laser is a flashlamp pumped with an Nd:YAG crystal coupled with a passive Q-switch with an output power density of about 10 MW/cm^2 and a weight of 3 kg. A laser driver and spectrometer were developed along with the laser. The spectrometer weighed approximately 2 kg and provided a resolution of 0.3 nm in the 480-560 nm spectral region. Exceptionally, it is composed of refractive optics instead of the usually used reflective optics, which is not associated with chromatic aberration. The instrument was successfully tested for the qualitative analysis of copper samples.

4.2. Commercial instruments

To the best of our knowledge, there are close to fifteen companies developing and providing commercial LIBS systems. Most of these companies offer bench-top LIBS instruments intended to be used in laboratory conditions and the majority of these instruments cannot be transported by one person. Tables 3 and 4 contain a list of eight selected companies offering portable LIBS instruments. The LIBSCAN 25 and Porta-LIBS-2000 portable LIBS devices are also presented in Table 2 and are reviewed in more detail below, as they relate to the published results.

One of the first commercially available portable LIBS instruments was the Porta-LIBS-2000 from the StellarNet Inc. Company [80,81]. The device was housed in a suitcase containing a small chamber in which the analyzed samples could be placed. Thanks to an incorporated trigger module, ten different delays between the laser shot and spectra detection could be selected to optimize the acquisition conditions. The device was used for preliminary studies in a laboratory [82] and for carbon [83] and copper [84] content determination in soil samples.

In [82], the instrument was used in the early stages of an experiment by using lab-made software for qualitative analyses, however without presenting any results for the portable system. In [83], Da Silva et al. used the device to determine carbon content in soil samples, applying univariate and multivariate linear regression (MLR) methods. Due to the strong interference of the C I 247.86 nm line with the neighboring iron lines, the C I 193.03 nm line was used. Linearities of $r = 0.95$ and $r = 0.97$ were obtained for the univariate and MLR, respectively. The MLR was found to be less influenced by the interference due to a close aluminum line. The authors pointed out the usefulness of portable LIBS instruments, even with low spectral resolution, for quantitative carbon measurements in soil.

The same research group also showed that the instrument could be used for quantitative copper determination in soil using an artificial neural network (ANN) [84]. They compared the results with the conventional linear calibration method. Fifty-nine Brazilian soil samples were used to determine the Cu content. For the conventional method, linearity was attained for the calibration curve with $r = 0.11$. For the ANN, two different selection strategies for the relevant wavelengths (ANN parameters) were experimented with, resulting in a linearity $r = 0.74$ and $r = 0.96$. The low linearity for the conventional method was attributed to the Cu line interfering with the neighboring lines of different elements, presented in the samples, which were indistinguishable due to the low spectral resolution of the spectrometer. However, interference was not so critical in the ANN-based analyses.

The second commercial portable LIBS system developed by Applied Photonics Ltd. is the LIBSCAN 25+. This instrument was used in several studies to analyze an ancient artifact [85], as part of a feasibility study to detect Home Made Explosive (HME) precursors [50] as well as to determine the origin of gun powder from gunshot residue (GSR) [86]. The common denominator for these studies was the treatment process for the acquired spectra. In all cases, the observation of the simple line intensity of given atomic transitions was used to reach specified objectives. In the first case (using the older, less powerful 20 mJ per pulse LIBSCAN 25 version), the transitions from Ag, Al, Au, Cu and Na were used to investigate the gilded silver alloy composition and to provide information about previous restoration treatments on the artifact [85]. For example, the in-depth analysis revealed the lack of copper in the surface layer which may be explained by an after-effect of a previous restoration. Miziolek [50] studied the spectra from ammonium nitrate and sodium chlorate in order to confirm that it is possible to differentiate between nitrates, chlorates and perchlorates with the LIBSCAN 25+ instrument. They concluded that the device may be a viable new tool, especially for HME-related materials. The same team also used this device for the GSR analysis [86]. In order to distinguish between three different gunpowder manufacturers, they followed the intensity variation of atomic lines from eight different elements: Ba, Ca, Au, Mg, K, Sr, Sn and Ti. Using the chemometric model (from StatPoint Technologies Inc., Warrenton, VA, USA), they were able to clearly separate two manufacturers, the last one with a probability of 80%. Together they reached an accuracy of 67%.

The effort to provide a real handheld LIBS device, used by a person with minimal training, by private companies appeared very recently. This is very encouraging and makes LIBS technology more accessible for those applications where high portability and fast analysis are crucial. As the handheld device is very limited in terms of its dimensions and weight, it places high demands on the instrumentation technological level and therefore it could advance the portable LIBS further ahead. It is worth mentioning that in the case of XRF technology, handheld devices have already been available on the market for a longer time. Table 4 provides a list of four companies and their handheld devices.

5. Portable LIBS instrumentation

In this section, the three most important parts of the portable LIBS system and their application are discussed. The requirements with regard to their compactness place limitations on their performance. However, there are some promising technologies.

5.1. Laser

As can be seen from Table 2 the Kigre MK-367 laser is very popular in the LIBS community and has been implemented in many devices [31,63,64,73,74,80,81,83,84,87,88]. It is an Nd:YAG FLPSS laser, lasing on 1064 nm. The laser is passively Q-switched, producing pulses with an energy up to 25 mJ at a maximum repetition rate of 1 Hz. The laser normally works in a single-pulse mode, but it can also produce a train of multiple pulses, separated by 20–30 μs, by applying higher voltage on the flashlamp [31,63]. The sum of energy in all of the pulses, in the multiple pulse operation mode, can be up to 175 mJ.

Table 3
List of the companies and commercial portable LIBS instruments with links to a description.

Company	Product name	Link to description
Applied Photonics Ltd.	LIBSCAN 25, 25+	http://www.appliedphotonics.co.uk/products_services/libscan_25.htm
Bertin Technologies	QUANTOM	http://www.bertin.fr/resources/fichiers/bertin/brochures/Quantom_FR.pdf
IVEA	EasyLIBS	http://www.ivea-solution.com/libs/product_info.php?cPath=25&products_id=50
StellarNet, Inc.	Porta-LIBS-2000	http://stellarnet-inc.com/public/download/StellarNet-PORTA-LIBS-SPEC.pdf

Table 4
List of the companies offering handheld portable LIBS devices with references.

Company	Product name	Link to description
Oxford Instruments	mPulse	http://www.oxford-instruments.com/products/analysers/handheld-analysers/handheld-libs-mpulse-scrap-metal-analyser
SciAps	Z500	http://sciaps.com/libz-take-tour/
TSI	CHEMLITE	http://www.tsi.com/ChemLite-Portable-LIBS-Metal-Analyzer/
Open Photonics		http://www.open-photonics.com/featured-technologies/handheld-libs-system

Compact FLPSS Nd:YAG lasers are commonly used in most of the developed portable devices; however, as will be presented, DPSS lasers could replace FLPSS lasers and increase the figure of merit of portable LIBS devices in the future. In fact, all of the devices presented in Table 2, except two, use the FLPSS laser. Although some improvements have been carried out to increase the energy of compact FLPSS laser up to 50 mJ per pulse [50,60,78,85,86] and to provide better synchronization with a detector by an active Q-switch, there are still some attributes that are difficult to improve, but which can be crucial for the performance of the portable LIBS device. Beam quality is one of those important parameters usually evaluated by the M^2 quantity [89], and which is equal to one for a perfect Gaussian beam. High beam quality allows for the production of small focal spots and therefore high fluences, inducing a more efficient breakdown and ablation of the material than for the lasers, producing low energy pulses. Additionally, beam quality is connected with a focus depth that is longer for a lower M^2 factor (higher beam quality) and shorter for a higher M^2 factor. The longer focus depth results in a lower fluence fluctuation and consequently lowers the sensitivity of the LIBS signal to the changes in the focusing lens–sample distance. As the precise definition of the distance could be problem in field applications, a longer focus depth is more desirable.

The repetition rate of the FLPSS, operating without an external cooling system, is usually limited to 1 Hz. All of the instruments housing the Kigre laser, presented here, work on an even lower repetition rate than its maximum because of the cooling requirements. When the accumulation of multiple pulses is used to investigate the same site of the sample, a higher repetition rate is desirable. It is not possible to hold the portable instrument in same position by hand for a long period of time and thus short measurement times are essential. Moreover, less time consuming measurements are very desirable in field operations. The cooling requirements are due to the heating of the gain medium of the laser. In FLPSS lasers, pumping with a spectrally wide flashlamp light is not as efficient and most of the light is turned into heat instead of pumping the gain medium [89]. When the gain medium is irradiated with a spectrally narrow light (like that from laser diodes in DPSS), the pumping process is more effective, less power consuming and less heat producing, resulting in higher repetition rates. Furthermore, effective pumping extends the operation lifetime of the device and reduces thermo-optic effects in the gain medium, resulting in better beam quality, smaller focal spots and higher fluences. For comparison, $M^2 < 2$ is common for the compact DPSS laser; however, it is difficult to reach $M^2 < 10$ for the compact FLPSS laser. For two beams with a M^2 factor of 2 and 10 and with 1 mJ and 25 mJ of energy per pulse, respectively, the resulting fluences will be equal. DPSS lasers can provide higher repetition rates, higher beam qualities and less power consumption in comparison with FLPSS lasers and they can be compact enough for implementation in portable LIBS instruments.

In the overview of the portable LIBS devices in Section 4 and Table 2, only two devices use a DPSS laser instead of a FLPSS laser [37,76]. Both lasers had repetition rates of 10 Hz and energies of 10 mJ and 14 mJ. In [23], an original FLPSS Kigre MK-367 laser was replaced by an Nd:YAG DPSS laser (model DP5120 from company JP Innovations) to decrease the measurement time. Even though the laser had small dimensions ($13.4 \times 8.7 \times 6.4$ cm) and was battery powered ($11 \times 6 \times 12.5$ cm), it was able to operate at a repetition rate of 10 Hz for at least 4 h. In the other instrument [10], the Kigre MK-830 DPSS laser was used. This laser is remarkable mainly due to a Er:glass gain medium, lasing on 1535 nm, making it an eye-safe laser.

The investigation into whether or not the DPSS laser can be applied to portable LIBS instruments has been presented in [67,90–92] under laboratory conditions. In [67,92], a very small passively Q-switched DPSS laser prototype was presented and compared with a laboratory FLPSS laser. The prototype laser was intended to be used in a LIBS device for a planetary surface mission with a maximum weight of 1 kg. The overall weight of the laser was 216 g with a laser head weight of 26 g. Both lasers, prototype and laboratory, had repetition rates of 10 Hz with pulse energies of 1.8 mJ and 40 mJ, respectively. Even with the large energy difference, the fluences were comparable (values of 66 J/cm^2 and 57 J/cm^2 for the prototype and laboratory laser, respectively) as the focal spot size of the DPSS laser was smaller. The study was carried out on geological samples (Martian analogue rocks) under simulated Martian atmospheric and surface conditions. All spectra were acquired by a non-gated detector. The resulted LODs ranged from 10 to 80 times higher (worse) for the DPSS laser prototype compared to the FLPSS laboratory laser. The precision was similar, from 10 to 20%, for both lasers. With respect to the very low weight and the performance of the laser, it can be considered as being very useful in portable LIBS instruments.

In [90], a prototype of an electronically Q-switched DPSS laser with a repetition rate of 8 kHz and an energy of 80 μJ per pulse was tested. The weight and dimensions of the laser were not mentioned, but it was referenced as a miniature laser with dimensions comparable to commercial compact microchip lasers (see Section 5.1.1). The laser was tested on aluminum samples with Mg, Fe, Mn, Ni, Cu, Ti and Si impurities. LIBS spectra were acquired by a gated and non-gated detector, resulting in LODs ranging from 2 to 7 times better for the non-gated detector compared to the gated detector (see Section 5.2.2). Moreover, the LODs for some elements were comparable to those obtained by laboratory LIBS systems [93,94]. The authors concluded that truly portable LIBS instruments could be built using the laser.

5.1.1. Microchip laser

For portable LIBS devices, there is an attractive subclass of DPSS lasers which comprises very compact microchip lasers [95,96]. The resonator of the microchip laser is very small and short, from one tenth of a millimeter to several millimeters, with mirrors directly coated onto the faces of an active laser crystal. Laser pulses are generated by passive Q-switching, by directly attaching a saturable absorber to the active crystal. By attaching harmonic conversion crystals to the absorber, higher-order harmonics for the fundamental laser wavelengths can be generated and the whole laser configuration will not exceed a couple of centimeters in size. Passive microchip lasers commonly operate in the fundamental transverse mode (TEM_{00}), producing high beam quality with a beam quality factor $M^2 < 1.3$. This allows for the production of a small focal spot and consequently, high irradiance levels on the sample surface. Due to the low pulse energies of microchip lasers, ranging from one to tens of μJ, a small focal spot is necessary to achieve breakdown. Hence, the focus of the microchip laser has to be tight and is usually produced by a microscope objective. The focus depth is therefore short and the properties of the plasma are more sensitive to changes in the sample-to-objective distance compared to a longer focus length used in high power lasers. As a result of the short resonator, the laser operates

in a single longitudinal mode, producing a single wavelength, preventing mode beating which can cause pulse to pulse variations in the LIBS emission signal [97]. Moreover, the short resonator generates short pulses lasting a few hundreds of ps (generally <1 ns). However, as pointed out by Cristoforetti et al. [90] (mentioned above), the short pulse duration can cause a lower LIBS signal. The repetition rates of microchip lasers are very high compared to the conventional FLPSS, ranging from one to tens of kHz. It can be adjusted by a changing the pumping power [98]. An overview of the application of microchip lasers in LIBS is shown in Table 5 and a more detailed description is found below.

The first use of microchip lasers for application in LIBS was presented in a master's thesis [99] concerned with the feasibility of microchip lasers in LIBS. The dependence of the quality of the LIBS signal on the laser repetition rate was studied in various Pb contaminated samples rotating during the experiment. The intensity of the LIBS signal per pulse decreased as the repetition rate increased; however, the S/N ratio increased. The signal decrease was related to the number of overlapped laser shots on the sample surface, increasing with the repetition rate. This behavior is common for microchip lasers working at high repetition rates.

In [97], the decrease in the signal was attributed to the higher breakdown threshold of a melt created on the surface of a sample due to the repetitive shooting to the same spot. If the repetition rate is too high, the melt cannot solidify before the next laser shot. Since microchip lasers provide high repetition rates, the decrease in the LIBS signal is common when shooting to the same spot. In order to maintain the intensity of the signal constant, the sample should move during the measurement. Due to the aforementioned high influence of the sample-focusing lens (objective) distance on plasma quality, the distance should stay constant during sample movement, which makes moving the sample even more complicated, especially in field applications.

For the microchip LIBS laser, the duration of the plasma light emission is similar to the duration of the laser pulse [97]. Due to the fast evolution of the plasma, gated detection is difficult and is further complicated by high jitter in the microchip laser [100,101]. Fortunately, plasma induced by microchip lasers produce a lower continuum than plasma induced by conventional lasers and therefore the emission can be detected by non-gated detectors [97,102–106], which are more suitable for the portable applications.

Ablation efficiency, defined as the ratio of the crater volume to the laser pulse energy ($\mu m^3/J$), is an important parameter and was observed at one order of magnitude greater for the microchip lasers ($2 \times 10^8\ \mu m^3/J$) than that obtained by conventional lasers ($2 \times 10^7\ \mu m^3/J$) with similar power densities [97]. The energy of the laser was 7 μJ and the high ablation efficiency was attributed to the high beam quality. However, it was impossible to detect Mg in a pelletized graphite powder for Mg contents under 20%. As the microchip laser used produced fluencies close to the breakdown threshold, the properties of the materials were found to be very important with regard to plasma induction. Different plasma properties can be expected for metals, semiconductors and insulators. The authors suggested the use of power chip lasers to extend the laser pulse energies.

In [104], a study on ablation efficiency was carried out with a 50 μJ high-power microchip ("powerchip") laser. The powerchip laser is a microchip laser with an increased cavity length producing higher output energies [107]. Curiously, a lower ablation efficiency for low melting point materials was presented and attributed to the re-deposition of the ablated material on the sample surface instead of vaporization and excitation. The heating test for the samples showed that lower thermal diffusion of incident pulse energy to the sample volume resulted in higher ablation efficiency. Although it is unreasonable to heat the sample for the portable LIBS instrument, it can be used for naturally hot samples, e.g. in the steel industry. The craters created by the microchip lasers were narrower and deeper in comparison to the 8 ns 0.5 mJ FLPSS laser on Pb targets and therefore mass removal can be quantified more precisely. Another investigation of powerchip feasibility was also presented in [105] by the same research group. In the spectroscopy studies, a non-gated detector with small compact spectrometers was used. The first shots were rejected due to a significant fluctuation in the LIBS signal. Calibration curves for Cr, Mn and Mo were built for the steel samples and the LOD were determined with values of 30, 40 and 90 ppm, respectively, and with an accuracy, in terms of RSD, of 3.6, 6.3 and 5.5%, respectively.

To overcome baseline noise and interference between neighboring lines, the multivariate calibration method (partial least squares — PLS) was used and compared with the standard univariate calibration method in [102,103]. For the study, a 14 μJ and 7.8 kHz repetition rate microchip laser and a non-gated and non-intensified small compact spectrometer were used. In [102], aluminum alloy samples were analyzed with the LOD determined for Fe, Mg, Mn, Ni, Si and Zn from 500 to 1400 ppm for the PLS analysis. All of the values were lower (better) compared with the standard univariate calibration method with the most significant differences for Si and Zn (more than ten times lower). However, the presented LODs were two orders of magnitude higher (worse) than those reached by the conventional laboratory LIBS apparatus.

In [103], steel samples were analyzed for carbon content by observing the spectral region around 193 nm. The LOD (2σ) of 400 ppm was reached by PLS analysis and 2400 ppm for the univariate calibration method. The authors concluded that it would be possible to build a handheld LIBS device for which high precision is not needed. The average relative error of prediction of 3.7 and 6.7% was obtained for Cr and Ni, respectively for PLS and 25.7 and 11.4%, respectively for the univariate analysis. The errors were comparable to those obtained for Ni and Cr in other works.

Although gated detectors are difficult to integrate into a portable device, it would be beneficial to mention some recent results for which powerchip lasers and ICCD were used together [100,101]. It is difficult to gate a passively Q-switched powerchip laser due to the short plasma duration and high jitter of the laser (7 μs). To overcome the 70 ns gate intersection delay of the ICCD, the detector was synchronized with the

Table 5
Overview of microchip and powerchip lasers used in LIBS experiments.

Ref.	Energy (μJ)	Duration (ps)	Rep. rate (kHz)	Spot (μm)	Fluence (J/cm^2)	Power density (GW/cm^2)	Application
[97]	7	550	5.45	8	14	25	Metallic foils: Cu, Fe, Ni, Pb, Sn, Ta, Ti, Zn Mg in pelletized graphite powder
[103]	14		7.8				Steel: C
[104]	7 50	500	5	8–10			Metallic foils: Al, Cu, Fe, Ni, Pb, Si wafer Cd
[105]	50	500	1	8–10			Steel: Cr, Mn, Mo, Ni, Si
[102]	14	500	7.8	20	4.7	9.4	Al alloy: Cu, Fe, Mg, Mn, Ni, Si, Zn
[106]	12	800	2				Steel: Cr, Ni
[100]	30	500	1				Al alloy: H
[101]	62 28[a]	500	1				Al alloy: Cu

[a] Second harmonics 532 nm.

laser pulse passing 25 m along an optical delay line.[1] Similarly, as pointed out by Cristoforetti et al. in [9,108], the results from the study [100] indicate that McWhirter's criteria are insufficient to assess the local thermodynamic equilibrium (LTE). The LTE condition is desired for calibration-free (CF) LIBS analyses; however, CF is not used in portable LIBS instruments due to high apparatus and data processing requirements. LOD of 14 and 1.29 ppm for copper in aluminum samples in air (10 and 0.65 in argon) were obtained with non-gated and gated detection, respectively [101]. It is worth noting that the duration of plasma generated by powerchip lasers is higher than the duration of plasma generated by microchip lasers, probably due to the higher energy.

5.1.2. Fiber laser

The other attractive laser sources for portable LIBS instruments are fiber lasers. The idea to use an optical fiber as the gain medium for a laser stretches back to the early 1960s [109,110], soon after the experimental demonstration of the first laser. These days, commercial fiber lasers, with appropriate dimensions and weight for use in a portable device, can produce pulses with energy that is high enough to initiate the breakdown and induce plasma on different materials. Due to their robustness, high repetition rate and high beam quality, fiber lasers are ideal sources for portable LIBS devices. However, until now, they have not been widely used in the LIBS community and only a couple of studies have been published on their use in LIBS [98,111–114]. The term fiber laser refers either to lasers with an optical fiber as the gain medium or to a fiber amplifier that is seeded by another laser (laser diode, microchip laser, etc.), termed a master oscillator fiber amplifier (MOFA). The core of the optical fiber is glass doped with rare-earth elements (Yb, Nd, Er, Tm), optically pumped, mostly, by laser diodes. The overview of the application of fiber lasers in LIBS is shown in Table 6 and they are described in further detail below.

Gravel et al. [113] investigated ablation by the MOFA fiber laser system and compared it to conventional FLPSS. The laser produced pulses with an energy of 800 μJ, duration of 30 ns at a repetition rate of 25 kHz. Using similar power densities for both lasers, fiber and FLPSS, the craters that appeared after ablation were compared by taking optical coherence tomography (OCT) and scanning electron microscopy (SEM) measurements. The fiber laser ablated deeper (7 μm per pulse) and more regular craters with a smaller diameter than the FLPSS laser (0.1 μm per pulse). Additionally, the dependence of crater depth on the shot number was linear for the first eight shots. A comparison of the craters for the high (25 kHz) and low (1 Hz) repetition rate operation suggested no inter-pulse effect for this kind of laser. The high ablation rate was attributed to the high beam quality and to the long pulse duration. It must be noted that Gornushkin et al. [97] used microchip laser producing pulses with a duration of 0.5 ns and with energies of 7 μJ, to gain a higher ablation efficiency (see Section 5.1.1). The higher LIBS signal attributed to the longer pulse duration was also presented by Cristoforetti et al. [90] by using the mini DPSS laser (see Section 5.1). In [113], an aluminum plasma plume life time was estimated at 6–8 microseconds and the plasma diameter ranged from 125–150 μm. Aluminum samples were analyzed for the composition of the Cr, Cu, Fe, Mg, Mn and Si elements with the LOD determined for a compact spectrometer of 10.8, 6.5, 210, 1.1, 4.4 and 82 ppm, respectively. The results are comparable with those obtained by conventional LIBS systems.

The amplification of a microchip laser's output pulse energy of 15 μJ to 600 μJ by the ytterbium fiber in the MOFA system and its application in a mobile LIBS device was presented in [98]. The aim of the device was to classify casing materials of mines and explosives in the field. The classification was based on the recognition of different decay times of the LIBS signal, for the C (248 nm) and CN (388 nm) spectral regions, for the different materials. The regions were spectrally filtered by bandpass filters and the signal was detected by a photomultiplier tube. For better analytical results, the ANN analysis was used. The different casing material was distinguished with 80% success; however, it was not possible to recognize the same kind of material, e.g. two different kind of plastics.

The same research group used a similar device, extended by a small compact spectrometer and an ANN combined with principal component analyses (PCA), for the identification of different materials by an unskilled person [111]. The Yb fiber laser, with a power density of 90 GW/cm^2, was found to not be powerful enough to produce a LIBS signal for TNT detection. The laboratory measurement showed that the minimum intensity for TNT detection was 200 GW/cm^2. However, by using Er:Yb fiber laser lasing at 1543.5 nm instead of Yb fiber laser lasing at 1064 nm, a much lower intensity with a value of 8 GW/cm^2 was found to be sufficient.

A thulium fiber laser lasing at a wavelength of 1992 nm, delivering energy pulses of 100 μJ with a 200 ns pulse duration, was used as a laser source for LIBS in [112]. LIBS spectra of a copper sample were detected and analyzed. Even in non-gated acquisition, the lack of a continuum and the absence of the O and N lines from air in the spectra were presented. The LTE condition was assessed and the temperature of the excitation states was determined to be 2.61 and 2.68 eV for neutrals and ions, respectively.

A 1.33 mJ pulse fiber laser with a repetition rate of 30 kHz was used to construct a mobile LIBS device for industrial application [114]. It was compared with a device based on spark-discharge emission spectroscopy (SD-OES) which was qualified as state-of-art technology. A decrease in the LIBS signal was observed after multiple shots to the same spot, but unlike the low energy microchip lasers, here the decrease is caused by material being removed from the focal spot. Due to the decrease in the signal, the sample was moved to a fresh focal spot after every 5 ms (150 pulses). The analytical result for aluminum and steel samples was similar for both technologies; however, the LIBS device was ten times less time-consuming than the SD-OES device.

The recent publication [61] is also from an industrial application and compares XRF and LIBS devices used to analyze metallic wear debris from machinery lubrication systems. A fiber laser producing pulses with an energy of 600 μJ and a duration of 200 ns was used as the laser source. For the spectral analyses, a small compact spectrometer covering the range from 220 to 480 nm with a resolution of 0.3 nm was used. The study suggests an advantage of the LIBS technique over the XRF technique mainly in the identification of aluminum alloys and titanium alloys containing light elements. With a 100% correct identification of all alloy samples and the possibility to design the device such that it weighs close to 15 kg indicates that fiber lasers have tremendous potential when applied to portable LIBS devices.

A special category of laser sources for LIBS comprises femtosecond (fs) lasers which produce ultrashort pulses with a duration in the order of hundreds of fs to a couple of ps. A comparison of fs lasers and nanosecond lasers has already been presented in several publications [39,115–119]. Usually, a mode locked Ti:sapphire laser is used [120–124] in the LIBS studies as an fs laser source. However, the Ti:sapphire laser is a complex and bulky device and it is only possible to use it under laboratory conditions. Closer to the topic of a field application for LIBS, studies using low energy Ti:sapphire fs lasers were also carried out [120,124,125]. For portable LIBS instruments, the generation of fs pulses by mode locking the fiber lasers appears to be more realistic [126,127]. Fs lasers interact differently with the sample surface than ns lasers. Whole energy is transferred to the material rapidly when the energy is not dissipated to a surrounding lattice and thus the material rapidly changes to ionized gas, resulting in a lower ablation threshold, higher ablation efficiency and the formation of a more regular crater [120].

Huang et al. [126] used commercial fs fiber laser lasing at 1030 nm, producing 750 fs pulses with energy and a repetition rate up to 10 μJ and 10 MHz, respectively, for LIBS studies. Metallic (aluminum, lead–tin alloy and brass), semiconductor (gallium–arsenide) and glass (soda lime glass) samples were examined by different energies and by moving the samples with various velocities. A comparison between gated and non-gated (ICCD and CCD) detection showed an S/N ratio that was

[1] For a more compact solution, it is suggested to use fiber.

Table 6
Overview of fiber lasers used in LIBS experiments.

Ref.	Energy (μJ)	Duration (ns)	Rep. rate (kHz)	Spot (μm)	Fluence (J/cm^2)	Power density (GW/cm^2)	Application
[113]	800	30	25	40	64		Aluminum, cooper Cr, Cu, Fe, Mg, Mn, Si
[98]	600	0.62	15	36	60	100	Explosives casing material C, CN
[111]	800	1.2	20	30		90	Different metals (coated, uncoated), explosives TNT Al, C, Ca, Cu, Fe, H, K, Mg, Na, Zn
[114]	1330	40	30				Aluminum, steel Co, Cr, Cu, Fe, Mg, Mn, Mo, Ni, Si, Si, Ti, V, W, Zn
[61]	600	200		30			Steel, titanium, nickel and aluminum alloys
[126][a]	0.750–3	750 fs	225	5			Metals, semiconductor, glass Al, As, Ca, Cu, K, Mg, Na, Pb, Sn, Zn
[127][a]	0.450	100 fs	2000				Brass, copper Cu, Zn

[a] Femtosecond laser.

20 times higher for gated detection. During the first 5 ns after the laser shot, a strong continuum was observed in the spectra with a poor line spectra structure for the aluminum sample. For the highest S/N ratio, the optimum detection window was determined from 10 to 30 ns. The energy threshold for plasma formation was observed at low energy (0.21 μJ) and the crater diameter after ablation was very small. For an energy of 0.39 μJ, the diameter was estimated at a value of 3.5 μm. In summary, it was found that the laser would be useful if incorporated into the portable LIBS device.

A developed fs fiber laser and its application in LIBS was presented in [127]. The laser produced 100 ps long clusters of pulses, with an energy of 450 nJ. The clusters are composed of short pulses with a duration of 100 fs and a repetition rate of 2 MHz. Brass and copper samples were used for a LIBS test, with a clear difference in terms of the presence and absence of Zn lines in the brass and copper sample, respectively. For the copper sample, a fluence threshold of 0.49 J/cm^2 was found to be extremely small in comparison to that obtained using other ns and fs lasers. The laser can be incorporated into the portable LIBS instrument and moreover, with the 14 W pump laser it can produce pulses with higher energy (3.9 μJ).

5.2. Spectrometer

The spectrometer is composed of two parts in order to analyze the incoming light and record the spectrum. The first part is comprised of the spectrograph — an optical system where the incoming light is decomposed as a function of its frequency. The second part includes the detector for measuring the intensity of the different light signal components.

5.2.1. Spectrograph

The Czerny–Turner design [128] of the spectrograph, in its various adaptations, is the most common choice among the described systems. Here, a single grating is used to disperse the incoming light over to a linear detector. Together with the Seya–Namioka design [129], where a confocal grating is used to reduce the number of collimating and focusing elements, these two designs are some of the simplest commercially available spectrographs. Both schemes possess the same limitation of linear dispersion spectrographs — they require having a detector that contains enough pixels to sample the dispersed signal in a single exposure. Currently, a common linear CCD array contains 1024 or 2048 pixels, limiting the spectral coverage and resolution to approximately 100 nm at 0.1 nm resolution per detector. In practice, this is nicely illustrated in Fig. 4, which also shows the resolution and single exposition bandwidth for each spectrograph. All of the devices except one use the Czerny–Turner configuration.

The simplest representations are in the II, IX, X and XI LIBS devices where the grating is fixed at given angle and the spectra are produced in a single range defined by the grating configuration (e.g. 2400 grooves/mm grating in II produces a spectrum that is 120 nm wide with a resolution of 0.4 nm). In the I, III and IV devices, the spectrographs allow for broader coverage by manually turning the grating, but the bandwidth is still limited for a single exposition, as seen in the previous cases. The simplest way to circumvent the spectral bandwidth limitations while keeping a high resolution is to install multiple spectrometric channels. This is the case for the V, VI (Porta-LIBS-2000 is available with two types of spectrometers, with 0.1 and 0.2 nm resolution, respectively), VII and VIII devices. The disadvantage of this approach is that is requires signal sampling into up to 7 channels (V and VI.b) in order to reach a resolution of 0.1 nm. In the XII device, Cremers et al. [76] used a different solution for the bandwidth problem. An echelle type spectrograph [130] was integrated into a backpack. In this configuration, the horizontally overlapping high diffraction orders of the echelle grating are separated vertically by a prism producing a 2D spectral image. Using a 2D array detector (like the CCD), it was possible to record these spectra simultaneously. In the XII device, the EMU-65 (from Catalina Scientific Instruments) was used to record the entire UV–VIS-NIR spectrum from 200 to 1000 nm with R = 44,000 in a single exposure.

If we look at all of the spectrographs used in the various LIBS devices together, we can see that all of the optical layouts are based on concepts that are over sixty years old (e.g. Czerny–Turner's article [128] was published in 1930 and the echelle article [130] appeared in 1949). In the following paragraph, we would like to point out a new “emerging” technology that may provide some perspectives with respect to future concepts of portable LIBS devices.

The Stationary-Wave Integrated Fourier Transform Spectrometer (SWIFT) [131] is a complete spectrometer system (spectrograph + detector) capable of achieving an ultra-high resolution (R = 50,000–70,000) in a very small package (8 × 2 × 20 cm for the bench-top version). This device is based on an idea used in 1891 by Gabriel Lippman for developing color photographs [132]. In the SWIFT spectrometer, light is focused into a waveguide finished by a fixed mirror. The interference pattern created is monitored through a set of gold nano-wires placed equidistantly across the waveguide. In the nano-wires, the evanescence field from the waveguide is transformed into photons. These photons are emitted to the detector array placed on the top of the waveguide. As the signal from the detector is under-sampled (the pitch of the pixels is usually greater than the distance between two nano-probes), a complex data analysis must be applied to transform the interferogram into a readable spectrum. The currently available devices (produced by Resolution Spectra Systems, www.resolutionspectra.com) produce a single shot bandwidth of approximately 100 nm (for a resolution of 0.01 nm) or approximately 10 nm for a resolution of 0.001 nm. This would, for example, give enough resolving power to distinguish between the different isotopic transitions, similarly to the case presented by Cremers et al. [76]. At the moment, the main disadvantage is that the range is limited to roughly 630 nm (Cremers et al. used transitions at around 421 nm to observe

different uranium isotopes). But ongoing development should enable shorter wavelengths in the near future.

5.2.2. Detector

The benchmark instruments for LIBS instruments are the array detectors (e.g. Charge Coupled Devices — CCD or Complementary Metal Oxide Semiconductors — CMOS) coupled with an intensifier unit (IU). This architecture offers both high signal amplification and precise full frame shuttering down to the nanosecond level suitable for monitoring LIP. They are the preferred choice of detector for most laboratory or bench-top LIBS devices. Although ICCDs with a weight under 1 kg (e.g. the XR/TURBO-EX from Stanford Photonics with a weight of 0.8 kg and measuring 127 × 65 × 61 mm in size) can be found on the market, the complexity of their design renders them unpractical for portable LIBS instruments. This comes from the fact that the IU is composed of elements that require a vacuum and high voltage to operate. Furthermore, the multiplication channels of the IU are fragile microstructures. Finally, the IU must be optically bound to the array detector (via focusing lenses or fiber taper). Altogether, this architecture possesses many structure weaknesses that may be a source of problems when working in the field. Therefore, in most portable LIBS instruments, the choice of detector falls to "single chip" structures such as the CCD.

A question concerning the quality of the detected spectra arises when using non-intensified and non-gated CCD detectors instead of gated ICCD detectors. In order to answer this question, a comparison between CCD and ICCD detectors was made in several studies [126,133–137]. In [134,136], the authors present a comparison between triggered CCD and ICDD detectors under different conditions. The results for the ICCD detector exhibited better S/N and LOD values compared to those obtained with the CCD detector. However, as pointed out in [135], the results can be different if both detectors would be evaluated under equal conditions. Thus, a new comparison was made and both types of detectors were tested with the same spectrograph and both were cooled. A mechanical chopper was used to trigger the CCD with jitter on the order of 100 ns. The CCD detector exhibited an S/N ratio and LOD comparable with those given by the ICCD detector. Generally, there is a higher possibility of optimizing the S/N ratio with the ICCD due to an adjustment of the integration time (gating) using small time steps (~10 ns). The time steps for the CCDs are much longer (in the order of ms) and they last longer than the characteristic time for the plasma emission decay.

However, more important than gating is the possibility for triggering as it allows for the delayed detection of the LIBS spectra with respect to the plasma ignition stage, in order to cut-off the strong continuum. The early stage of the plasma is very hot and therefore a strong continuum dominates in the emission spectra due to prevailing free electron transitions. Moreover, high temperature plasma is a source of noise from various origins and unstable spectral lines corresponding to ionic species [133]. Therefore, when the early plasma stage is included in time integrated spectra, it negatively influences the S/N and S/B ratios [63,135]. Hence, a certain delay time after plasma ignition must be used before spectra detection. In [4], the S/N ratios for a delay of 0 and 100 ns were 0.5 and 1.6, respectively, although the intensity of the line decreased just to 90% for a 100 ns delay with respect to the 0 ns delay.

As presented above, a triggered CCD can attain comparable S/N and LOD values to the ICCD under identical experimental conditions. The delay in spectra detection in portable LIBS instruments is commonly provided by using linear CCDs [59,63,69,134,136,138,139]. They allow for fast triggering by draining (resetting) the detector's content just before exposure to detected light. The trigger can be affected by jitter, e.g. 250, 100 and 42 ns in [136,134] and [139], respectively, and can negatively influence the S/N ratio. However, new CCD detectors have already reduced the amount of jitter. An intrinsic delay from 1 μs to 10 μs must be taken into account after resetting the CCD. If the intrinsic delay is too long and the laser is not actively Q-switched, the laser has to be triggered to some event before the laser pulse rather than to the laser pulse event itself, e.g. to the laser's flash lamp. In the case of actively Q-switched lasers, the trigger for the detector can simply occur before the laser pulse with the possibility to adjust the optimum delay.

It must also be noted that some alternative possibilities to obtain time resolved spectra with CCDs have been presented in [140] and [133]. In [140], the triggering was carried out by using an acousto-optic modulator. In [133], spatial resolution was exchanged with temporal resolution in plasma analyses. The results were comparable to those obtained with the gated detector. Another possibility to obtain gated spectra is to detect spectra for two different delays and to subtract one from the other when the integration time is the difference between the two delays. It is also worth mentioning that, by implementing electronic shutter technology, linear CCDs provide gating with an integration time down to 2 μs (Hamamatsu S11155-2048-01). Such time ranges are starting to be interesting for temporally resolved LIBS. When a 2D array detector is needed (e.g. for echelle or SWIFT type spectrographs), a similar performance could be produced by Frame Interline Transfer (FIT) CCDs. Each pixel of the FIT detectors has an additional blinded storage pixel used at the end of the exposition time for the simultaneous transfer of the accumulated charge to this pixel. For example, the company PCO offers this detector (pco.ultraviolet) with exposition times from 1 μs (with a weight of 0.35 kg and a size of 80 × 50 × 50 mm).

Nowadays, two principal state of the art technologies for detectors competing on the market: Electron Multiplying CCDs (EM-CCD) and Scientific CMOS (S-CMOS) detectors. In the EM-CCD detectors, a multiplication register is added into the chip in order to amplify the accumulated charge before it is read by the read-out amplifier. The S-CMOS represents an evolution of the CMOS architecture. In the CMOS detectors, each pixel has its own amplifier allowing a parallel read-out of the accumulated charge. Originally, the cost of the parallel read-out capability was the different gain, linearity and noise level of each amplifier, thus high read-out noise. These attributes are strongly diminished in the S-CMOS devices due to the advanced architecture of the read-out circuit. Compared to the ICCD, both the EM-CCD and S-CMOS have a critical advantage with regard to portable applications as they are both "single chip" structures. On the other hand, especially in the case of the EM-CCD, the EM does not offer any triggering capabilities, for example like the IU in the ICCD.

Based on the different noise sources in each architecture (e.g. by Butch Moomaw in [141]), it was possible to use the S/N ratio to compare the performance for a given detected photon count (light intensity) per read-out. For the smallest detected photon counts, the EM-CCD or ICCD cameras offer the best S/N ratio. These values are better than in the CCD or S-CMOS but due to the excess noise present in the multiplication register or in the IU, the shot-noise limit (SNL) could not be attained. This is achieved by S-CMOS devices for counts close to 20 photons per readout. A cooled CCD needs approximately 1000 photons to attain the SNL. For higher intensities, the cooled CCD is capable of maintaining the SNL, whereas in the S-CMOS cameras (from approximately 1500 photons per read-out) the pixel fluctuation noise draws the S/N ratio from the SNL. If we consider the comparison with respect to the total photon flux, the quantum efficiency of each detector must be taken into account. Here, the best performance is offered by back-thinned detectors (CCDs or EM-CCDs) with values over 90% for specific wavelengths. They are followed by the S-CMOS, with values over 70% using the micro-lens technology. It should be noted that the cost of using these improvements lies in the sensitivity cut-off for the UV part of the spectrum (this technology is also used in some FIT CCDs to increase their efficiency in the visible part of the spectra). ICCDs have the worst quantum efficiency due to the photon—electron—photon conversion process (around 40%).

The dimension and weight of these cameras becomes an important issue when investigating their possible integration into LIBS devices. Currently, there are S-CMOS cameras weighing less than 1 kg on the market. For example, Raptor Photonics (Osprey) and PCO (edge 5.5) offer a couple of cameras. These cameras weigh 0.5 kg and 0.7 kg for dimensions of 86 × 65 × 62 mm and 89 × 70 × 62 mm, respectively.

In both cases, there is a global shutter that allows for the simultaneous exposition of all pixels. The minimum exposition times are 33 and 10 μs, respectively. The heavier camera sold by PCO has a better dynamic range (88.6 dB versus 65 dB) and lower readout noise (1 e^- versus 7 e^-). In both cases, the spectral range is limited to about 330 nm due to the micro-lens array. In the case of the EM-CCDs, the problem is that most of the devices on the market are quite heavy (approximately 3 kg) and they are too bulky to be considered for a possible integration. An interesting option is to look for FIT EM-CCDs in order to have better shutter control (e.g. Kite EM-CCD from Raptor Photonics with a weight less than 0.6 kg).

6. Discussion

Most of the new laser sources presented above produce pulses with much lower energy than conventional small FLPSS lasers. The energy difference is most significant for microchip lasers, for which the energy per pulse can be three orders of magnitude lower than the energy of small FLPSS lasers commonly used in portable LIBS devices. Although the energy in the pulse is much lower, the power (the sum of energy delivered by the laser within one second) and the power density in the focal spot are comparable. However, the properties of plasma induced by the microchip lasers are different. The LODs published for microchip lasers are two orders of magnitude lower compared to conventional FLPSS laboratory lasers, suggesting that the low energy, even for a high quality beam, can be a problem. This is not the case with small DPSS and fiber lasers, which have higher output energy and power that is comparable with the FLPSS lasers used in the laboratory. The reviewed LODs of these lasers are comparable with those used in laboratory LIBS systems, suggesting that their performance is higher compared to small FLPSSs. Microchip lasers, even with low LOD, can be used to construct really small and light portable LIBS devices where the dimensions and weight are more critical than the performance.

The production of a small continuum by the microchip and fiber lasers allows for the use of non-gated and non-triggered spectra detection, thereby making the construction of portable devices less complicated and less expensive. However, the high continuum of FLPSS lasers can be cut-off by triggering the detector, with delayed exposition with respect to the onset of the laser. However, for precise timing, the laser should be actively Q-switched.

The high ablation efficiency, low breakdown thresholds and nicely shaped small-diameter craters, after laser ablation, suggest the use of microchip and fiber laser for precise punctual analyses. However, this is probably useless when the laser probe is held in the hand. Additionally, for low homogeneity samples, spatial integration would be greatly appreciated, but the increase of the focus spot is limited due to the breakdown threshold and low energy per pulse. From this point of view, the small FLPSS lasers that produced more energetic pulses can be used to investigate a larger surface area in one pulse.

The biggest drawback of the small FLPSS lasers is their low repetition rate. This limits the number of spectra obtained within a set time period, which may extend the time needed for a measurement. Conversely, the high repetition rate of the microchip and fiber lasers results in the detection of a lot of spectra during a short time period but the number of accumulated spectra is limited by the fast decrease in the plasma emission intensity. To maintain a certain intensity in the plasma emission, the sample must be moved. This feature makes it more complicated to use high repetition lasers. However, the decrease in the signal must be determined for specific laser and sample types as it might not be critical with sufficient spectra quality, even without sample movement.

There are also small DPSS lasers with energies just slightly lower than the energies of the FLPSS lasers, allowing for a repetition rate that is approximately ten times higher. Reference [76] illustrates a simple example of this: by simply replacing the FLPSS laser by the DPSS laser, the measurement time can decrease rapidly due to a repetition rate that is thirty times higher, something that is impossible to achieve with the small FLPSS laser.

In the case of the spectrometers that are the most suitable for portable LIBS instruments, weight and size represent the main limitations for the selection criteria. Currently, only echelle design spectrographs offer the capability of recording the whole spectrum from UV to IR with the necessary resolution; however, they are bulky devices that weigh over 5 kg. Moreover, they require a 2D array detector which results in another series of complications (e.g. the size of the packaging and the gating of the detector). In the near future, SWIFT spectrographs may become an interesting alternative, but for now, the most reasonable choice seems to be the Czerny–Turner design single or multiple spectrograph(s) coupled with a linear detector.

Regarding the detector itself, the first selection criterion is its dimensions. As previously mentioned for the Czerny-Turner spectrograph, the linear CCD is a very convenient choice. But when a 2D array detector is needed, there are more options to choose from. When considering both the S/N ratio and size/power criteria, simple FIT CCDs appear to be the best alternative. This comes from the fact that LIP is an intense source of radiation; therefore, even for small exposition times, there are many photons for the CCD to reach the SNL. The EM-CCD or ICCD would only give better results (in the S/N ratio) if there are fewer than 1000 detected photons per exposition. Although the FIT design for the CCD would not have the same gating possibilities as the ICCD, for most LIBS applications, the microsecond-scale for exposition is sufficient. In the near future, when the micro-lens array will be made from UV transparent material, the S-CMOS may become an interesting alternative to the FIT CCD design as, in addition to microsecond gating capabilities, they would also offer a faster frame rate allowing for faster spectra recording.

7. Conclusion

In this review, the developed portable LIBS devices and their applications have been presented together with the new laser sources used in LIBS. Only portable LIBS instruments are presented that can be transported by one person without a car or a trolley and that are powered by batteries and weigh up to 15 kg. These devices exhibit a lot of advantages compared to their strongest competitor, XRF devices; however, the XRF is still the technology of the choice in many applications. The reason for this could be due to the lower performance and lower portability of LIBS devices, which can be improved with the use of the new technologies for their instrumentation. The compact FLPSS laser source is used in most devices. The review of the new small DPSS, microchip and fiber lasers in LIBS applications suggests that they can provide better properties for future portable LIBS instruments. In particular, small DPSS and fiber lasers can reach high levels of performance that can be compared with bulky laboratory FLPSS lasers. New lasers offer a better power to weight or dimension ratio, they are more efficient and less power consuming, which is what makes them preferable for portable LIBS applications. With regard to the spectrometers, technological improvements are mainly noticeable due to the detectors, which are now faster and more sensitive. Although SWIFT spectrometers are limited to longer wavelengths (>630 nm), ongoing development should enable shorter wavelengths in the near future and new spectrometers with a higher resolution could possibly replace standard compact spectrometers.

There are still challenges in the instrumentation of portable LIBS devices. However, the already existing technology makes the development of a truly portable and reliable device possible.

Acknowledgment

We would like to acknowledge support from the Grant Agency of the Czech Republic, project number 13-11635S.

References

[1] M. Baudelet, B.W. Smith, The first years of laser-induced breakdown spectroscopy, J. Anal. At. Spectrom. 28 (2013) 624, http://dx.doi.org/10.1039/c3ja50027f.
[2] D.A. Cremers, L.J. Radziemski, Handbook of Laser-Induced Breakdown Spectroscopy, Wiley, 2013.
[3] A.W. Miziolek, V. Palleschi, I. Schechter, Laser Induced Breakdown Spectroscopy, Cambridge University Press, 2006.
[4] Y.-I. Lee, K. Song, J. Sneddon, Laser-Induced Breakdown Spectrometry, Nova Publishers, 2000.
[5] J.P. Singh, S.N. Thakur, Laser-Induced Breakdown Spectroscopy, Elsevier Science, 2007.
[6] S. Musazzi, U. Perini (Eds.), Laser-Induced Breakdown Spectroscopy, Theory and Applications, Springer, 2014.
[7] R. Noll, Laser-Induced Breakdown Spectroscopy: Fundamentals and Applications, Springer, 2012.
[8] L.J. Radziemski, D.A. Cremers, Lasers-Induced Plasmas and Applications, CRC Press, 1989.
[9] G. Cristoforetti, E. Tognoni, L.A. Gizzi, Thermodynamic equilibrium states in laser-induced plasmas: from the general case to laser-induced breakdown spectroscopy plasmas, Spectrochim. Acta Part B 90 (2013) 1–22, http://dx.doi.org/10.1016/j.sab.2013.09.004.
[10] A. De Giacomo, M. Dell'Aglio, R. Gaudiuso, S. Amoruso, O. De Pascale, Effects of the background environment on formation, evolution and emission spectra of laser-induced plasmas, Spectrochim. Acta Part B 78 (2012) 1–19, http://dx.doi.org/10.1016/j.sab.2012.10.003.
[11] F. Fortes, J. Laserna, The development of fieldable laser-induced breakdown spectrometer: no limits on the horizon, Spectrochim. Acta Part B 65 (2010) 975–990, http://dx.doi.org/10.1016/j.sab.2010.11.009.
[12] F.J. Fortes, J. Moros, P. Lucena, L.M. Cabalín, J.J. Laserna, Laser-induced breakdown spectroscopy, Anal. Chem. 85 (2013) 640–669, http://dx.doi.org/10.1021/ac303220r.
[13] R. Gaudiuso, M. Dell'Aglio, O. De Pascale, G.S. Senesi, A. De Giacomo, Laser induced breakdown spectroscopy for elemental analysis in environmental, cultural heritage and space applications: a review of methods and results, Sensors (Basel) 10 (2010) 7434–7468, http://dx.doi.org/10.3390/s100807434.
[14] A. Giakoumaki, K. Melessanaki, D. Anglos, Laser-induced breakdown spectroscopy (LIBS) in archaeological science—applications and prospects, Anal. Bioanal. Chem. (2007) 749–760, http://dx.doi.org/10.1007/s00216-006-0908-1.
[15] I.B. Gornushkin, U. Panne, Radiative models of laser-induced plasma and pump-probe diagnostics relevant to laser-induced breakdown spectroscopy, Spectrochim. Acta Part B 65 (2010) 345–359, http://dx.doi.org/10.1016/j.sab.2010.03.021.
[16] D.W. Hahn, N. Omenetto, Laser-induced breakdown spectroscopy (LIBS), part I: review of basic diagnostics and plasma–particle interactions: still-challenging issues within the analytical plasma community, Appl. Spectrosc. 64 (2010) 335–366, http://dx.doi.org/10.1366/000370210793561691.
[17] D.W. Hahn, N. Omenetto, Laser-induced breakdown spectroscopy (LIBS), part II: review of instrumental and methodological approaches to material analysis and applications to different fields, Appl. Spectrosc. 66 (2012) 347–419, http://dx.doi.org/10.1366/11-06574.
[18] R. Harmon, R. Russo, R. Hark, Applications of laser-induced breakdown spectroscopy for geochemical and environmental analysis: a comprehensive review, Spectrochim. Acta Part B 87 (2013) 11–26, http://dx.doi.org/10.1016/j.sab.2013.05.017.
[19] M. Khater, Laser-induced breakdown spectroscopy for light elements detection in steel: state of the art, Spectrochim. Acta Part B 81 (2013) 1–10, http://dx.doi.org/10.1016/j.sab.2012.12.010.
[20] M.A. Khater, Trace detection of light elements by laser-induced breakdown spectroscopy (LIBS): applications to non-conducting materials, Opt. Spectrosc. 115 (2013) 574–590, http://dx.doi.org/10.1134/S0030400X13100123.
[21] A. Michel, Review: applications of single-shot laser-induced breakdown spectroscopy, Spectrochim. Acta Part B 65 (2010) 185–191, http://dx.doi.org/10.1016/j.sab.2010.01.006.
[22] C. Pasquini, J. Cortez, L.M.C. Silva, F.B. Gonzaga, Laser induced breakdown spectroscopy, J. Braz. Chem. Soc. 18 (2007) 463–512, http://dx.doi.org/10.1590/S0103-50532007000300002.
[23] L. Radziemski, D. Cremers, A brief history of laser-induced breakdown spectroscopy: from the concept of atoms to LIBS 2012, Spectrochim. Acta Part B 87 (2013) 3–10, http://dx.doi.org/10.1016/j.sab.2013.05.013.
[24] D.A. Rusak, B.C. Castle, B.W. Smith, J.D. Winefordner, Fundamentals and applications of laser-induced breakdown spectroscopy, Crit. Rev. Anal. Chem. 27 (1997) 257–290, http://dx.doi.org/10.1080/10408349708050587.
[25] B. Sallé, P. Mauchien, S. Maurice, Laser-Induced Breakdown Spectroscopy in open-path configuration for the analysis of distant objects, Spectrochim. Acta Part B 62 (2007) 739–768, http://dx.doi.org/10.1016/j.sab.2007.07.001.
[26] V.K. Singh, A.K. Rai, Prospects for laser-induced breakdown spectroscopy for biomedical applications: a review, Lasers Med. Sci. 26 (2011) 673–687, http://dx.doi.org/10.1007/s10103-011-0921-2.
[27] K. Song, Y.-I. Lee, J. Sneddon, Recent developments in instrumentation for laser induced breakdown spectroscopy, Appl. Spectrosc. Rev. 37 (2002) 89–117, http://dx.doi.org/10.1081/ASR-120004896.
[28] E. Tognoni, V. Palleschi, Quantitative micro-analysis by laser-induced breakdown spectroscopy: a review of the experimental approaches, Spectrochim. Acta Part B 57 (2002) 1115–1130.
[29] J. Winefordner, I. Gornushkin, Comparing several atomic spectrometric methods to the super stars: special emphasis on laser induced breakdown spectrometry, LIBS, a future super star, J. Anal. At. Spectrom. (2004) 1061–1083.
[30] C. Aragón, J.A. Aguilera, Characterization of laser induced plasmas by optical emission spectroscopy: a review of experiments and methods, Spectrochim. Acta Part B 63 (2008) 893–916.
[31] K.Y. Yamamoto, D.A. Cremers, M.J. Ferris, L.E. Foster, Detection of metals in the environment using a portable laser-induced breakdown spectroscopy instrument, Appl. Spectrosc. 50 (1996) 222–233, http://dx.doi.org/10.1366/0003702963906519.
[32] J. Cuñat, F.J. Fortes, L.M. Cabalín, F. Carrasco, M.D. Simón, J.J. Laserna, Man-portable laser-induced breakdown spectroscopy system for in situ characterization of karstic formations, Appl. Spectrosc. 62 (2008) 1250–1255.
[33] J. Cuñat, F.J. Fortes, J.J. Laserna, Real time and in situ determination of lead in road sediments using a man-portable laser-induced breakdown spectroscopy analyzer, Anal. Chim. Acta. 633 (2009) 38–42, http://dx.doi.org/10.1016/j.aca.2008.11.045.
[34] F.J. Fortes, T. Ctvrtnícková, M.P. Mateo, L.M. Cabalín, G. Nicolas, J.J. Laserna, Spectrochemical study for the in situ detection of oil spill residues using laser-induced breakdown spectroscopy, Anal. Chim. Acta. 683 (2010) 52–57, http://dx.doi.org/10.1016/j.aca.2010.09.053.
[35] F.J. Fortes, J. Cuñat, L.M. Cabalín, J.J. Laserna, In situ analytical assessment and chemical imaging of historical buildings using a man-portable laser system, Appl. Spectrosc. 61 (2007) 558–564.
[36] F.J. Fortes, I. Vadillo, H. Stoll, M. Jiménez-Sánchez, A. Moreno, J.J. Laserna, Spatial distribution of paleoclimatic proxies in stalagmite slabs using laser-induced breakdown spectroscopy, J. Anal. At. Spectrom. 27 (2012) 868, http://dx.doi.org/10.1039/c2ja10299d.
[37] M.J. Myers, J.D. Myers, J.T. Sarracino, C.R. Hardy, B. Guo, S.M. Christian, J.A. Myers, F. Roth, A.G. Myers, LIBS system with compact fiber spectrometer, head mounted spectra display and hand held eye-safe erbium glass laser gun, in: W.A. Clarkson, N. Hodgson, R.K. Shori (Eds.), Solid State Lasers XIX Technol. Devices, 10.1117/12.841901, 2010, (pp. 75782G-75782G-16).
[38] L.M. Cabalín, J.J. Laserna, Experimental determination of laser induced breakdown thresholds of metals under nanosecond Q-switched laser operation, Spectrochim. Acta Part B 53 (1998) 723–730, http://dx.doi.org/10.1016/S0584-8547(98)00107-4.
[39] A. Semerok, C. Chaléard, V. Detalle, Experimental investigations of laser ablation efficiency of pure metals with femto, pico and nanosecond pulses, Appl. Surf. Sci. (1999) 311–314.
[40] D. Bäuerle, Laser Processing and Chemistry, Springer Berlin Heidelberg, Berlin, Heidelberg, 2011., http://dx.doi.org/10.1007/978-3-642-17613-5.
[41] NIST Atomic Spectra Database, http://www.nist.gov/pml/data/asd.cfm.
[42] R.L. Kurucz, B. Bell, 1995 Atomic line data (Kurucz CD-ROM No. 23), Smithsonian Astrophysical Observatory, Cambridge, MA, 1996. (http://www.cfa.harvard.edu/amp/ampdata/kurucz23/sekur.html).
[43] J. Lam, V. Motto-Ros, D. Misiak, C. Dujardin, G. Ledoux, D. Amans, Investigation of local thermodynamic equilibrium in laser-induced plasmas: measurements of rotational and excitation temperatures at long time scales, Spectrochim. Acta Part B (2014), http://dx.doi.org/10.1016/j.sab.2014.07.013.
[44] J.A. Aguilera, C. Aragón, Characterization of laser-induced plasma during its expansion in air by optical emission spectroscopy: observation of strong explosion self-similar behavior, Spectrochim. Acta Part B 97 (2014) 86–93, http://dx.doi.org/10.1016/j.sab.2014.04.013.
[45] J.A. Pérez-Serradilla, A. Jurado-López, M.D. Luque de Castro, Complementarity of XRFS and LIBS for corrosion studies, Talanta 71 (2007) 97–102, http://dx.doi.org/10.1016/j.talanta.2006.03.034.
[46] M. Ferretti, G. Cristoforetti, In situ study of the Porticello Bronzes by portable X-ray fluorescence and laser-induced breakdown spectroscopy, Spectrochim. Acta Part B 62 (2007) 1512–1518, http://dx.doi.org/10.1016/j.sab.2007.09.004.
[47] L. Pardini, A. El Hassan, M. Ferretti, X-Ray Fluorescence and Laser-Induced Breakdown Spectroscopy analysis of Roman silver denarii, Spectrochim. Acta Part B 74–75 (2012) 156–161, http://dx.doi.org/10.1016/j.sab.2012.06.016.
[48] X. Hou, B. Jones, Field instrumentation in atomic spectroscopy, Microchem. J. 66 (2000) 115–145.
[49] R.F. LeBouf, A.L. Miller, C. Stipe, J. Brown, N. Murphy, A.B. Stefaniak, Comparison of field portable measurements of ultrafine TiO_2: X-ray fluorescence, laser-induced breakdown spectroscopy, and Fourier-transform infrared spectroscopy, Environ. Sci. Process. Impacts 15 (2013) 1191–1198, http://dx.doi.org/10.1039/c3em00108c.
[50] A.W. Miziolek, Progress in fieldable laser-induced breakdown spectroscopy (LIBS), in: M.A. Druy, R.A. Crocombe (Eds.), SPIE Defense, Secur. Sens, 10.1117/12.919492International Society for Optics and Photonics, 2012, (pp. 837402-837402-13).
[51] S. Bichlmeier, K. Janssens, J. Heckel, D. Gibson, P. Hoffmann, H.M. Ortner, Component selection for a compact micro-XRF spectrometer, X-Ray Spectrom. 30 (2001) 8–14, http://dx.doi.org/10.1002/xrs.457.
[52] G. Vittiglio, S. Bichlmeier, P. Klinger, J. Heckel, W. Fuzhong, L. Vincze, K. Janssens, P. Engström, A. Rindby, K. Dietrich, D. Jembrih-Simbürger, M. Schreiner, D. Denis, A. Lakdar, A. Lamotte, A compact μ-XRF spectrometer for (in situ) analyses of cultural heritage and forensic materials, Nucl. Inst. Methods Phys. Res. Sect. B Beam Interact. Mater. Atoms 213 (2004) 693–698, http://dx.doi.org/10.1016/S0168-583X(03)01687-2.
[53] L. Bonizzoni, S. Caglio, A. Galli, G. Poldi, Comparison of three portable EDXRF spectrometers for pigment characterization, X-Ray Spectrom. 39 (2010) 233–242, http://dx.doi.org/10.1002/xrs.1253.
[54] H. Bronk, S. Röhrs, A. Bjeoumikhov, N. Langhoff, J. Schmalz, R. Wedell, H.-E. Gorny, A. Herold, U. Waldschläger, ArtTAX — a new mobile spectrometer for energy-dispersive micro X-ray fluorescence spectrometry on art and archaeological objects, Fresenius J. Anal. Chem. 371 (2014) 307–316, http://dx.doi.org/10.1007/s002160100989.
[55] A.S. Eppler, D.A. Cremers, D.D. Hickmott, M.J. Ferris, A.C. Koskelo, Matrix effects in the detection of Pb and Ba in soils using laser-induced breakdown spectroscopy, Appl. Spectrosc. 50 (1996) 1175–1181.

[56] R.A. Multari, L.E. Foster, D.A. Cremers, M.J. Ferris, Effect of sampling geometry on elemental emissions in laser-induced breakdown spectroscopy, Appl. Spectrosc. 50 (1996) 1483–1499, http://dx.doi.org/10.1366/0003702963904593.

[57] V. Sturm, H.-U. Schmitz, T. Reuter, R. Fleige, R. Noll, Fast vacuum slag analysis in a steel works by laser-induced breakdown spectroscopy, Spectrochim. Acta Part B 63 (2008) 1167–1170, http://dx.doi.org/10.1016/j.sab.2008.08.004.

[58] V. Sturm, Optical micro-lens array for laser plasma generation in spectrochemical analysis, J. Anal. At. Spectrom. 22 (2007) 1495, http://dx.doi.org/10.1039/b708564h.

[59] R.A. Myers, N.J. Kolodziejski, M.R. Squillante, Commercialization of laser-induced breakdown spectroscopy for lead-in-paint inspection, Appl. Opt. 47 (2008) G7–G14.

[60] J. Rakovský, O. Musset, J. Buoncristiani, V. Bichet, F. Monna, P. Neige, P. Veis, Testing a portable laser-induced breakdown spectroscopy system on geological samples, Spectrochim. Acta Part B 74–75 (2012) 57–65, http://dx.doi.org/10.1016/j.sab.2012.07.018.

[61] P. Suresh, Portable, real-time alloy identification of metallic wear debris from machinery lubrication systems: laser-induced breakdown spectroscopy versus x-ray fluorescence, 9101 (2014) 91010K, http://dx.doi.org/10.1117/12.2053056.

[62] B.C. Castle, A.K. Knight, K. Visser, B.W. Smith, J.D. Winefordner, Battery powered laser-induced plasma spectrometer for elemental determinations, J. Anal. At. Spectrom. 13 (1998) 589–595.

[63] R.T. Wainner, R.S. Harmon, A.W. Miziolek, K.L. McNesby, P.D. French, Analysis of environmental lead contamination: comparison of LIBS field and laboratory instruments, Spectrochim. Acta Part B 56 (2001) 777–793, http://dx.doi.org/10.1016/S0584-8547(01)00229-4.

[64] R.S. Harmon, F.C. De Lucia, A.W. Miziolek, K.L. McNesby, R.A. Walters, P.D. French, Laser-induced breakdown spectroscopy (LIBS) — an emerging field-portable sensor technology for real-time, in-situ geochemical and environmental analysis, Geochem. Explor. Environ. Anal. 5 (2005) 21–28, http://dx.doi.org/10.1144/1467-7873/03-059.

[65] B. Bousquet, G. Travaillé, A. Ismaël, L. Canioni, K. Michel-Le Pierrès, E. Brasseur, S. Roy, I. le Hecho, M. Larregieu, S. Tellier, M. Potin-Gautier, T. Boriachon, P. Wazen, A. Diard, S. Belbèze, Development of a mobile system based on laser-induced breakdown spectroscopy and dedicated to in situ analysis of polluted soils, Spectrochim. Acta Part B 63 (2008) 1085–1090, http://dx.doi.org/10.1016/j.sab.2008.09.008.

[66] C. Lopez-Moreno, S. Palanco, J. Laserna, Remote laser-induced plasma spectrometry for elemental analysis of samples of environmental interest, J. Anal. At. Spectrom. (2004) 1479–1484.

[67] S.G. Pavlov, E.K. Jessberger, H.-W. Hübers, S. Schröder, I. Rauschenbach, S. Florek, J. Neumann, H. Henkel, S. Klinkner, Miniaturized laser-induced plasma spectrometry for planetary in situ analysis — the case for Jupiter's moon Europa, Adv. Space Res. 48 (2011) 764–778, http://dx.doi.org/10.1016/j.asr.2010.06.034.

[68] F.C. DeLucia, A.C. Samuels, R.S. Harmon, R.A. Walters, K.L. McNesby, A. LaPointe, R.J. Winkel, A.W. Miziolek, Laser-induced breakdown spectroscopy (LIBS): a promising versatile chemical sensor technology for hazardous material detection, IEEE Sensors J. 5 (2005) 681–689, http://dx.doi.org/10.1109/JSEN.2005.848151.

[69] R.S. Harmon, F.C. DeLucia, C.E. Mcmanus, N.J. McMillan, T.F. Jenkins, M.E. Walsh, A. Miziolek, Laser-induced breakdown spectroscopy — an emerging chemical sensor technology for real-time field-portable, geochemical, mineralogical, and environmental applications, Appl. Geochem. 21 (2006) 730–747, http://dx.doi.org/10.1016/j.apgeochem.2006.02.003.

[70] R.S. Harmon, F.C. De Lucia, A. LaPointe, A.W. Miziolek, Man-portable LIBS for landmine detection, Proc. SPIE 6217 (2006), http://dx.doi.org/10.1117/12.667564 (62170I-62170I-7).

[71] J. Cuñat, S. Palanco, F. Carrasco, Portable instrument and analytical method using laser-induced breakdown spectrometry for in situ characterization of speleothems in karstic caves, J. Anal. At. Spectrom. (2005) 295–300.

[72] S. Palanco, A. Alises, J. Cuñat, J. Baena, J.J. Laserna, Development of a portable laser-induced plasma spectrometer with fully-automated operation and quantitative analysis capabilities, J. Anal. At. Spectrom. 18 (2003) 933, http://dx.doi.org/10.1039/b303248e.

[73] J.E. Barefield, S.M. Clegg, D.K. Veirs, L.N. Lopez, L.A. Le, M. Browne, L. Lopez, Application of Laser Induced Breakdown Spectroscopy (LIBS) instrument for international safeguards, INMM 51st Annu. Meet., Los Alamos, 2010, pp. 0–11.

[74] J.E. Barefield, S.M. Clegg, S.A. La Montagne, K.D. Veal, L. Le, L. Lopez, Development of Laser Induced Breakdown Spectroscopy instrumentation for safeguards applications, IAEA Symp. Int. Safeguards, Vienna, Austria, IAEA-CN-184/134, 2010.

[75] D.A. Cremers, R.C. Chinni, M. Bostian, L.J. Radziemski, C. Navarro-Northrup, C.R. Jones, L. Karch, Detection of actinide elements using LIBS, Proc. Inst. Nucl. Mater., 2010.

[76] D.A. Cremers, A. Beddingfield, R. Smithwick, R.C. Chinni, C.R. Jones, B. Beardsley, L. Karch, Monitoring uranium, hydrogen, and lithium and their isotopes using a compact Laser-Induced Breakdown Spectroscopy (LIBS) probe and high-resolution spectrometer, Appl. Spectrosc. 66 (2012) 250–261.

[77] M.J. Myers, J.D. Myers, B. Guo, C. Yang, C.R. Hardy, J.A. Myers, A.G. Myers, S.M. Christian, Non-invasive in-situ detection of malignant skin tissue and other abnormalities using portable LIBS system with fiber spectrometer and eye-safe, in: G.L. Coté, A.V. Priezzhev (Eds.), Biomed. Opt. 2008, 10.1117/12.764685International Society for Optics and Photonics, 2008, (pp. 68630W-68630W-10).

[78] J. Goujon, A. Giakoumaki, V. Piñon, O. Musset, D. Anglos, E. Georgiou, J.P. Boquillon, A compact and portable laser-induced breakdown spectroscopy instrument for single and double pulse applications, Spectrochim. Acta Part B 63 (2008) 1091–1096, http://dx.doi.org/10.1016/j.sab.2008.08.019.

[79] O. Ormachea, O. Urquidi, D. Casazola, Development of a portable low-cost LIBS system, in: M.F.P.C. Martins Costa (Ed.), 8th Iberoam. Opt. Meet. 11th Lat. Am. Meet. Opt. Lasers, Appl. 10.1117/12.2025507, 2013, p. 87851D.

[80] W. Pierce, S.M. Christian, M.J. Myers, J.D. Myers, C.R. Hardy, J.A. Myers, R. Gadson, W. Younis, Field-testing for environmental pollutants using briefcase sized portable LIBS system, LIBS_2004, 3rd Int. Conf. Laser Induc. Plasma Spectrosc. Appl., 2004, pp. 1–14.

[81] W. Pierce, S.M. Christian, Portable LIBS instrumentation can identify trace levels of environmental pollutants, Photonik (2006) 92–94.

[82] E. Yurdanur-Tasel, H. Berberoglu, S. Bilikmen, Investigation of materials of different crystal structure under various time delays using double pulse laser induced breakdown spectroscopy, Spectrochim. Acta Part B 74–75 (2012) 74–79, http://dx.doi.org/10.1016/j.sab.2012.07.006.

[83] M. Robson, D.M.B.P. Milori, E.C. Ferreira, E.J. Ferreira, F.J. Krug, L. Martin-Neto, Total carbon measurement in whole tropical soil sample, Spectrochim. Acta Part B 63 (2008) 1221–1224, http://dx.doi.org/10.1016/j.sab.2008.09.003.

[84] E.C. Ferreira, D.M.B.P. Milori, P. Mauchien, E.J. Ferreira, R.M. Da Silva, L. Martin-Neto, Artificial neural network for Cu quantitative determination in soil using a portable Laser Induced Breakdown Spectroscopy system, Spectrochim. Acta Part B 63 (2008) 1216–1220.

[85] M. Grozeva, P. Penkova, In Situ LIBS Analysis of Valuable Museum Objects: The Mogilanska Tumulus Ritual Knemida, Issp.bas.bg., 2012. 103–107.

[86] E. Hondrogiannis, D. Andersen, A.W. Miziolek, The evaluation of a new technology for gunshot residue (GSR) analysis in the field, SPIE Def. Secur. Sens. 8726 (2013) 87260P, http://dx.doi.org/10.1117/12.2017900.

[87] I.B. Gornushkin, B.W. Smith, H. Nasajpour, J.D. Winefordner, Identification of solid materials by correlation analysis using a microscopic laser-induced plasma spectrometer, Anal. Chem. 71 (1999) 5157–5164, http://dx.doi.org/10.1021/ac9905524.

[88] J.M. Anzano, I.B. Gornushkin, B.W. Smith, J.D. Winefofdner, J.D. Winefordner, Laser-induced plasma spectroscopy for plastic identification, Polym. Eng. Sci. 40 (2000) 2423–2429, http://dx.doi.org/10.1002/pen.11374.

[89] W. Koechner, Solid-State Laser Engineering, Springer, 2006.

[90] G. Cristoforetti, S. Legnaioli, V. Palleschi, A. Salvetti, E. Tognoni, P. Alberto Benedetti, F. Brioschi, F. Ferrario, A. Benedetti, Quantitative analysis of aluminium alloys by low-energy, high-repetition rate laser-induced breakdown spectroscopy, J. Anal. At. Spectrom. 21 (2006) 697–702, http://dx.doi.org/10.1039/b604628b.

[91] C. Wagner, J. Ewald, G. Ankerhold, P. Kohns, Non-metal elemental analysis by a compact low-energy high-repetition rate laser-induced-breakdown spectrometer, in: P.H. Lehmann (Ed.), Proc. SPIE, 10.1117/12.825054International Society for Optics and Photonics, 2009, p. 738929.

[92] I. Rauschenbach, E.K. Jessberger, S.G. Pavlov, H.-W. Hübers, Miniaturized Laser-Induced Breakdown Spectroscopy for the in-situ analysis of the Martian surface: calibration and quantification, Spectrochim. Acta Part B 65 (2010) 758–768, http://dx.doi.org/10.1016/j.sab.2010.03.018.

[93] M.A. Ismail, G. Cristoforetti, S. Legnaioli, L. Pardini, V. Palleschi, A. Salvetti, E. Tognoni, M. a Harith, Comparison of detection limits, for two metallic matrices, of laser-induced breakdown spectroscopy in the single and double-pulse configurations, Anal. Bioanal. Chem. 385 (2006) 316–325.

[94] W. Mohamed, Improved LIBS limit of detection of Be, Mg, Si, Mn, Fe and Cu in aluminum alloy samples using a portable Echelle spectrometer with ICCD camera, Opt. Laser Technol. 40 (2008) 30–38, http://dx.doi.org/10.1016/j.optlastec.2007.04.004.

[95] J.J. Zayhowski, A. Mooradian, Single-frequency microchip Nd lasers, Opt. Lett. 14 (1989) 24–26.

[96] J.J. Zayhowski, Passively Q-switched Nd:YAG microchip lasers and applications, J. Alloys Compd. 304 (2000) 393–400.

[97] I.B. Gornushkin, K. Amponsah-Manager, B.W. Smith, N. Omenetto, J.D. Winefordner, Microchip laser-induced breakdown spectroscopy: a preliminary feasibility investigation, Appl. Spectrosc. 58 (2004) 762–769, http://dx.doi.org/10.1366/0003702041389427.

[98] C. Bohling, D. Scheel, K. Hohmann, W. Schade, M. Reuter, G. Holl, Fiber-optic laser sensor for mine detection and verification, Appl. Opt. 45 (2006) 3817–3825.

[99] G.M.H. Hwang, Feasibility Study of Micro-Laser Induced Breakdown Spectroscopy Applied to Lead Identification in Metal Alloys and Environmental Matrices, Massachusetts Institute of Technology, 1998.

[100] J.A. Merten, B.W. Smith, N. Omenetto, Local thermodynamic equilibrium considerations in powerchip laser-induced plasmas, Spectrochim. Acta Part B 83–84 (2013) 50–55, http://dx.doi.org/10.1016/j.sab.2013.01.011.

[101] J.A. Merten, E. Ewusi-Annan, B.W. Smith, N. Omenetto, Optimizing gated detection in high-jitter kilohertz powerchip laser-induced breakdown spectroscopy, J. Anal. At. Spectrom. 29 (2014) 571, http://dx.doi.org/10.1039/c3ja50348h.

[102] A. Freedman, F.J. Iannarilli, J.C. Wormhoudt, Aluminum alloy analysis using microchip-laser induced breakdown spectroscopy, Spectrochim. Acta Part B 60 (2005) 1076–1082, http://dx.doi.org/10.1016/j.sab.2005.03.020.

[103] J. Wormhoudt, F.J. Iannarilli, S. Jones, K.D. Annen, A. Freedman, Determination of carbon in steel by laser-induced breakdown spectroscopy using a microchip laser and miniature spectrometer, Appl. Spectrosc. 59 (2005) 1098–1102, http://dx.doi.org/10.1366/0003702055012528.

[104] K. Amponsah-Manager, N. Omenetto, B.W. Smith, I.B. Gornushkin, J.D. Winefordner, Microchip laser ablation of metals: investigation of the ablation process in view of its application to laser-induced breakdown spectroscopy, J. Anal. At. Spectrom. 20 (2005) 544, http://dx.doi.org/10.1039/b419109a.

[105] C. Lopez-Moreno, K. Amponsah-Manager, B.W. Smith, I.B. Gornushkin, N. Omenetto, S. Palanco, J.J. Laserna, J.D. Winefordner, Quantitative analysis of low-alloy steel by microchip laser induced breakdown spectroscopy, J. Anal. At. Spectrom. 20 (2005) 552, http://dx.doi.org/10.1039/b419173k.

[106] F. Barbieri, C. Pasquini, A compact and low cost laser induced breakdown spectroscopic system: application for simultaneous determination of chromium and nickel in steel using multivariate calibration, Spectrochim. Acta Part B 69 (2012) 20–24, http://dx.doi.org/10.1016/j.sab.2012.02.007.

[107] J.J. Zayhowski, Microchip lasers, Opt. Mater. (Amst.) 11 (1999) 255–267.

[108] G. Cristoforetti, A. De Giacomo, M. Dell'Aglio, S. Legnaioli, E. Tognoni, V. Palleschi, N. Omenetto, Local thermodynamic equilibrium in Laser-Induced Breakdown Spectroscopy: beyond the McWhirter criterion, Spectrochim. Acta Part B 65 (2010) 86–95, http://dx.doi.org/10.1016/j.sab.2009.11.005.
[109] E. Snitzer, Optical maser action of Nd^{+3} in a barium crown glass, Phys. Rev. Lett. 7 (1961) 444–446, http://dx.doi.org/10.1103/PhysRevLett.7.444.
[110] E. Snitzer, Proposed fiber cavities for optical masers, J. Appl. Phys. 32 (1961) 36, http://dx.doi.org/10.1063/1.1735955.
[111] C. Bohling, K. Hohmann, D. Scheel, C. Bauer, W. Schippers, J. Burgmeier, U. Willer, G. Holl, W. Schade, All-fiber-coupled laser-induced breakdown spectroscopy sensor for hazardous materials analysis, Spectrochim. Acta Part B 62 (2007) 1519–1527, http://dx.doi.org/10.1016/j.sab.2007.10.038.
[112] M. Baudelet, C.C.C. Willis, L. Shah, M. Richardson, Laser-induced breakdown spectroscopy of copper with a 2 μm thulium fiber laser, Opt. Express 18 (2010) 7905–7910.
[113] J.-F.Y. Gravel, F.R. Doucet, P. Bouchard, M. Sabsabi, Evaluation of a compact high power pulsed fiber laser source for laser-induced breakdown spectroscopy, J. Anal. At. Spectrom. 26 (2011) 1354, http://dx.doi.org/10.1039/c0ja00228c.
[114] M. Scharun, C. Fricke-Begemann, R. Noll, Laser-induced breakdown spectroscopy with multi-kHz fibre laser for mobile metal analysis tasks — a comparison of different analysis methods and with a mobile spark-discharge optical emission spectroscopy apparatus, Spectrochim. Acta Part B 87 (2013) 198–207, http://dx.doi.org/10.1016/j.sab.2013.05.007.
[115] V. Margetic, A. Pakulev, A. Stockhaus, A comparison of nanosecond and femtosecond laser-induced plasma spectroscopy of brass samples, Spectrochim. Acta Part B (2000) 1771–1785.
[116] M. Baudelet, L. Guyon, J. Yu, J.-P. Wolf, T. Amodeo, E. Fréjafon, P. Laloi, Femtosecond time-resolved laser-induced breakdown spectroscopy for detection and identification of bacteria: a comparison to the nanosecond regime, J. Appl. Phys. 99 (2006) 084701, http://dx.doi.org/10.1063/1.2187107.
[117] Y. Dikmelik, C. McEnnis, J.B. Spicer, Femtosecond and nanosecond laser-induced breakdown spectroscopy of trinitrotoluene, Opt. Express 16 (2008) 5332–5337.
[118] J.-B. Sirven, B. Bousquet, L. Canioni, L. Sarger, Time-resolved and time-integrated single-shot laser-induced plasma experiments using nanosecond and femtosecond laser pulses, Spectrochim. Acta Part B 59 (2004) 1033–1039, http://dx.doi.org/10.1016/j.sab.2004.05.009.
[119] G.W. Rieger, M. Taschuk, Y.Y. Tsui, R. Fedosejevs, Comparative study of laser-induced plasma emission from microjoule picosecond and nanosecond KrF-laser pulses, Spectrochim. Acta Part B 58 (2003) 497–510, http://dx.doi.org/10.1016/S0584-8547(03)00014-4.
[120] F.C. De Lucia, J.L. Gottfried, A.W. Miziolek, Evaluation of femtosecond laser-induced breakdown spectroscopy for explosive residue detection, Opt. Express 17 (2009) 419–425.
[121] W. Liu, H.L. Xu, G. Méjean, Y. Kamali, J.-F. Daigle, A. Azarm, P.T. Simard, P. Mathieu, G. Roy, S.L. Chin, Efficient non-gated remote filament-induced breakdown spectroscopy of metallic sample, Spectrochim. Acta Part B 62 (2007) 76–81, http://dx.doi.org/10.1016/j.sab.2007.01.001.
[122] D.J. Hwang, H. Jeon, C.P. Grigoropoulos, J. Yoo, R.E. Russo, Femtosecond laser ablation induced plasma characteristics from submicron craters in thin metal film, Appl. Phys. Lett. 91 (2007) 251118, http://dx.doi.org/10.1063/1.2825289.
[123] H.L. Xu, G. Méjean, W. Liu, Y. Kamali, J.-F. Daigle, A. Azarm, P.T. Simard, P. Mathieu, G. Roy, J.-R. Simard, S.L. Chin, Remote detection of similar biological materials using femtosecond filament-induced breakdown spectroscopy, Appl. Phys. B 87 (2006) 151–156, http://dx.doi.org/10.1007/s00340-006-2536-z.
[124] A.W. Schill, D.A. Heaps, D.N. Stratis-Cullum, B.R. Arnold, P.M. Pellegrino, Characterization of near-infrared low energy ultra-short laser pulses for portable applications of laser induced breakdown spectroscopy, Opt. Express 15 (2008) 14044–14056.
[125] M.T. Taschuk, S.E. Kirkwood, Y.Y. Tsui, R. Fedosejevs, Quantitative emission from femtosecond microplasmas for laser-induced breakdown spectroscopy, J. Phys. Conf. Ser. 59 (2007) 328–332, http://dx.doi.org/10.1088/1742-6596/59/1/069.
[126] H. Huang, L.-M. Yang, J. Liu, Qualitative assessment of laser-induced breakdown spectra generated with a femtosecond fiber laser, Appl. Opt. 51 (2012) 8669–8676.
[127] B. Nie, G. Parker, V.V. Lozovoy, M. Dantus, Energy scaling of Yb fiber oscillator producing clusters of femtosecond pulses, Opt. Eng. 53 (2013) 051505, http://dx.doi.org/10.1117/1.OE.53.5.051505.
[128] M. Czerny, A.F. Turner, Uber den Astigmatismus bei Spiegelspektrometern, Z. Phys. 61 (1930) 792–797, http://dx.doi.org/10.1007/BF01340206.
[129] T. Namioka, Theory of the Concave Grating III Seya-Namioka Monochromator, J. Opt. Soc. Am. 49 (1959) 951, http://dx.doi.org/10.1364/JOSA.49.000951.
[130] G.R. Harrison, The production of diffraction gratings: II. The design of echelle gratings and spectrographs, J. Opt. Soc. Am. 39 (1949) 522, http://dx.doi.org/10.1364/JOSA.39.000522.
[131] E. le Coarer, S. Blaize, P. Benech, I. Stefanon, A. Morand, G. Lérondel, G. Leblond, P. Kern, J.M. Fedeli, P. Royer, Wavelength-scale stationary-wave integrated Fourier-transform spectrometry, Nat. Photonics 1 (2007) 473–478, http://dx.doi.org/10.1038/nphoton.2007.138.
[132] G. Lippmann, C. R. Acad. Sci. (Paris) 112 (1891) 274.
[133] V. Bulatov, R. Krasniker, I. Schechter, Converting spatial to pseudotemporal resolution in laser plasma analysis by simultaneous multifiber spectroscopy, Anal. Chem. 72 (2000) 2987–2994.
[134] J.E. Carranza, E. Gibb, B.W. Smith, D.W. Hahn, J.D. Winefordner, Comparison of nonintensified and intensified CCD detectors for laser-induced breakdown spectroscopy, Appl. Opt. 42 (2003) 6016, http://dx.doi.org/10.1364/AO.42.006016.
[135] M. Mueller, I.B. Gornushkin, S. Florek, D. Mory, U. Panne, Approach to detection in laser-induced breakdown spectroscopy, Anal. Chem. 79 (2007) 4419–4426, http://dx.doi.org/10.1021/ac0621470.
[136] M. Sabsabi, R. Héon, L. St-Onge, Critical evaluation of gated CCD detectors for laser-induced breakdown spectroscopy analysis, Spectrochim. Acta Part B 60 (2005) 1211–1216, http://dx.doi.org/10.1016/j.sab.2005.05.030.
[137] M.T. Taschuk, Y. Godwal, Y.Y. Tsui, R. Fedosejevs, M. Tripathi, B. Kearton, Absolute characterization of laser-induced breakdown spectroscopy detection systems, Spectrochim. Acta Part B 63 (2008) 525–535, http://dx.doi.org/10.1016/j.sab.2008.01.004.
[138] J. Goujon, O. Musset, A. Giakoumaki, V. Pinon, D. Anglos, E. Georgiou, A new compact laser source for portable LIBS applications, Proc. SPIE 6871 (2008), http://dx.doi.org/10.1117/12.777953 (68712Q-68712Q-11).
[139] J. Agresti, A.A. Mencaglia, S. Siano, Development and application of a portable LIPS system for characterising copper alloy artefacts, Anal. Bioanal. Chem. 395 (2009) 2255–2262, http://dx.doi.org/10.1007/s00216-009-3053-9.
[140] T. Sakka, K. Irie, K. Fukami, Y.H. Ogata, Emission spectroscopy of laser ablation plasma with time gating by acousto-optic modulator, Rev. Sci. Instrum. 82 (2011) 023112, http://dx.doi.org/10.1063/1.3544021.
[141] B. Moomaw, Camera Technologies for Low Light Imaging: Overview and Relative Advantages, 4th ed. Elsevier Inc., 2013.